Université de Montréal

Linking Dissolved Organic Matter Quality and Quantity to CO_2 and CH_4 Concentrations in Ombrotrophic Bog Pools

Par

Mahmud Hassan

Département de sciences biologiques

Faculté des arts et des sciences

Mémoire présenté en vue de l'obtention du grade de

Maître ès sciences (M.Sc.) en sciences biologiques

Juin 2022

Université de Montréal

Faculté des supérieures et postdoctorales

Ce mémoire intitulé

Relier la composition et la concentration de la matière organique dissoute aux concentrations de CO_2 et CH_4 dans les mares de tourbières

Présenté par

Mahmud Hassan

Sera évalué par un jury composé des personnes suivantes

Jacques Brisson

Président-rapporteur

Jean-François Lapierre

Directeur de recherche

Julie Talbot

Co-directrice de recherche

Tonya DelSontro

Examinatrice externe

Résumé

Les petits plans d'eau, en particulier ceux riches en matière organique, sont encore négligés en tant que sources naturelles majeures d'émission de carbone (C) dans l'atmosphère et contributeurs importants au bilan mondial de C. Les mares de tourbières riches en matières organiques sont une source nette de C atmosphérique dans les écosystèmes de tourbières, qui sont généralement un puits net de C. Ces mares émettent des gaz à effet de serre (GES) à des taux plus élevés, en particulier de méthane (CH_4), par rapport à d'autres petits plans d'eau lentiques (petits lacs et étangs), ce qui peut être attribué à la connectivité hydraulique des bassins donc aux apports en C de la tourbe environnante et aux caractéristiques morphologiques des mares. Cependant, il existe très peu d'informations sur les schémas et les mécanismes de la dynamique du C dans les bassins de tourbières par rapport à leur couvert végétal ainsi qu'à d'autres petits environnements aquatiques. En particulier, la matière organique dissoute (MOD), un important intermédiaire et substrat de C, peut influencer la dynamique des émissions de GES, mais son rôle demeure méconnu à l'échelle intra- et inter-régionale. Dans cette étude, nous avons caractérisé et identifié les patrons intra- et interrégionaux et les mécanismes potentiels contrôlant la quantité et la qualité de la MOD et des concentrations de GES, ainsi que leurs liens en analysant une gamme de variables optiques et chimiques et en compilant les données géographiques (c'est-à-dire le climat, le couvert végétal et morphométrie des bassins) à partir de bassins de tourbières ombrotrophes dans cinq régions de l'est du Canada (Grande plée Bleue, sud du Québec et région de la Minganie, est du Québec) et du sud de la Patagonie chilienne (Punta Arenas, parc Karukinka et île Navarino). Nous avons également effectué un échantillonnage interannuel dans la Grande plée Bleue pour identifier les tendances temporelles des concentrations et de la composition des GES et de MOD. Nous avons trouvé une variabilité interrégionale élevée dans les patrons de MOD et de GES par rapport à la variabilité intrarégionale qui était cohérente avec l'hétérogénéité des propriétés géographiques, en particulier, le climat. Les patrons interrégionaux des concentrations de GES étaient de plus déterminés par la couverture végétale environnante, la morphométrie du bassin et la composition de la MOD de type protéique. D'autre part, bien que nous n'ayons pas observé de patrons temporels significatifs dans les concentrations de GES, de MOD et de la composition de type humique terrestre au cours de l'été dans la Grande plée Bleue, les patrons temporels de GES ont été influencés par la concentration de MOD, la composition de type humique terrestre, et la chimie interne de l'eau. Dans l'ensemble, nos résultats suggèrent que les patrons interrégionaux de la MOD

et des GES, et les liens entre eux, sont principalement contrôlés par le climat (température et précipitations), la couverture végétale et la morphométrie des bassins, tandis que les patrons temporels de la MOD et des GES sont principalement régis par des facteurs à l'échelle locale tels que la morphométrie des bassins et la connectivité hydrologique.

Mots clés : Cycle du carbone, petits plans d'eau, tourbières, mares, climat, biogéochimie, matière organique dissoute, gaz à effet de serre.

Abstract

Small waterbodies, especially organic-rich, are still overlooked as a major natural source of carbon (C) emission to the atmosphere and an important contributor in the global C budget. Organic-rich peatland pools are generally net atmospheric C sources embedded in peatland ecosystems, which are generally net C sinks. They emit high areal rates of greenhouse gases (GHG), particularly methane (CH_4), compared to other small lentic waterbodies (small lakes and ponds) which may be attributed to peat-pool hydraulic connectivity leading to C loading from the surrounding peat and morphological characteristics. But there is very little information on the patterns and drivers of C dynamics within peatland pools compared to their vegetated areas as well as other small aquatic environments. In particular, the role that dissolved organic matter (DOM), an important intermediate and C substrate, may play in GHG dynamics is poorly known at the intra- and inter-regional scales. In this study, we characterized and identified the intra- and inter regional patterns and drivers of DOM quantity and quality and GHG concentrations as well as their links. We did so by analyzing a range of optical and chemical variables and compiling geographic data (i.e., climate, vegetation cover and pool morphometry) from ombrotrophic peatland pools across five regions in eastern Canada (Grande plée Bleue, southern Québec and Minganie region, eastern Québec) and southern Chilean Patagonia (Punta Arenas, Karukinka Park and Navarino Island). We also conducted inter-annual sampling in Grande plée Bleue to identify the temporal patterns in GHG and DOM concentrations and composition. We found high inter-regional variability in DOM and GHG patterns compared to intra-regional variability which was coherent with the heterogeneity of geographical properties. Inter-regional patterns in GHG concentrations were driven by surrounding vegetation cover, pool morphometry and protein-like DOM composition. On the other hand, although we did not observe significant temporal patterns in GHG and DOM concentrations and terrestrial humic-like composition throughout the growing seasons in Grande plée Bleue, temporal patterns of GHG were influenced by the DOM concentration, terrestrial humic-like composition, and internal water chemistry. Overall, our results suggest that inter-regional patterns in DOM and GHG, and the links among them are predominantly controlled by the broad-scale patterns in climate (temperature and precipitation), vegetation cover, and pool morphometry, while temporal patterns in DOM and GHG are predominantly governed by local-scale drivers such as pool morphometry.

Keywords: Carbon cycle, small waterbodies, peatland pools, climate, water chemistry, dissolved organic matter, greenhouse gases.

Table of contents

List of tables

List of figures

List of acronyms and abbreviations

ANOVA: Analysis of variance

cal. y BP: Calibrated years before present

CH_4: Methane

CO_2: Carbon dioxide

CRU TS: Climatic Research Unit gridded Time Series

DOC: Dissolved organic carbon

DOM: Dissolved organic matter

GC: Gas chromatography

GHG: Greenhouse gas

GPB: Grande plée Bleue

GPS: Global positioning system

H_2SO_4: Sulfuric acid

MG: Minganie

IC: Inorganic carbon

KK: Karukinka

LOWESS: Locally-weighted scatterplot smoothing

M: Molar concentration

MAP: Mean annual precipitation

MAT: Mean annual temperature

NaOH: Sodium hydroxide

NI: Navarino Island

NPP: Net primary production

NH_4^+: Ammonia

NO_3^-: Nitrate

OM: Organic matter

p: p-value

PA: Punta Arenas

PARAFAC: Parallel factor analyses

PE: Polyethylene

PES: Polyethersulfone

PLSR: Partial least squares regressions

PO_4^{3-}: Phosphate

R^2: Correlation coefficient

SD: Standard deviation

SUVA: Specific ultraviolet absorbance

TC: Total carbon

TIC: Total inorganic carbon

TN: Total nitrogen

TOC: Total organic carbon

TP: Total phosphorus

USEPA: United States Environmental Protection Agency

UV: Ultraviolet

VIP: Variable importance in projection

YSI: Yellow spring instrument

To my late parents

Acknowledgment

This project would not have been possible without the help of many people. First, I would like to express my gratitude and deepest sense of appreciation and heartiest gratefulness to my honorable Supervisor and Co-supervisor Dr. Jean-François Lapierre, Associate Professor, Département de sciences biologiques, Université de Montréal and Dr. Julie Talbot, Associate Professor, Département de Géographie, Université de Montréal, for their scholastic guidance, unwavering support, valuable instruction, consecutive suggestion, constant encouragement and generosity of time and knowledge throughout the research work.

I wish to express my deepest sincere thankfulness to Julien Arsenault, Ph.D. candidate of Talbot lab and Lapierre lab for sampling design, sample collection from ombrotrophic bogs located in southern and eastern Québec, Canada, and three Chilean Patagonian regions (Punta Arenas, Karukinka, and Navarino Island), and laboratory analysis. My special thanks to our Chilean collaborators (Karla Martinez-Cruz, Armando Sepulveda-Jauregui and Jorge Hoyos-Santillan) who contributed a lot of data and expertise for the Chilean sampling.

I express gratitude and thanks to Dominic Bélanger for laboratory support. Thanks to all my lab mates at Lapierre lab and Talbot lab for their necessary help and inspiration throughout the period of the study.

Chapter 1: General Introduction

1.1 Context

Small waterbodies (i.e., streams, lakes, and ponds) represent a major, but still overlooked contributor in the global carbon (C) budget (Mullins & Doyle, 2019). This major contribution results from high areal rates of greenhouse gases (GHG) emission to the atmosphere, combined with high cumulative area worldwide. Particularly, organic-rich small waterbodies emit more GHG, especially methane (CH_4), to the atmosphere than other small waterbodies (Wik et al., 2016; Rosentreter et al., 2021; Kuhn et al., 2021) and are abundant across northern peatlands (Messager et al., 2016). For example, peatland ponds (pools) emit almost seven times more CH_4 (~15% of total CH_4 flux during the ice-free period) to the atmosphere than any other small lentic waterbodies (i.e., small lakes and ponds) in the northern hemisphere (Wik et al., 2016). However, the internal and external processes and the drivers controlling the high production and fluxes of carbon dioxide (CO_2) and CH_4 in small waterbodies are still not well understood. Hypothesized reasons behind the high C evasion from small lentic waterbodies compared to larger systems are high terrigenous C loading, high perimeter to area ratio, low water depth, frequent mixing (Holgerson 2015; Holgerson & Raymond, 2016), and hydrological connectivity between terrestrial and aquatic parts (McKenzie et al., 2021; Kuhn et al., 2021). Only a few studies have been done to identify the drivers of C fluxes in small lentic waterbodies (e.g., Natchimuthu et al., 2014; Holgerson, 2015; Webb et al., 2019; Peacock et al., 2019; Kuhn et al., 2021). Hence, knowledge of the main controls on C dynamics, and in particular, the role that dissolved organic matter (DOM) may play in GHG dynamics is limited. Better understanding DOM patterns with contrasting geographical properties (i.e., climate, topography, morphometry, and vegetation cover) and their links with GHG dynamics is important because DOM is an important intermediate and C source in the C cycle.

1.2 Global C fluxes from small waterbodies

There is no formal definition of "small waterbodies" (Biggs et al., 2017) regarding their specific size range and role in aquatic ecosystems (Mullins and Doyle, 2019). Regardless of the definition, it is clear that despite relatively low global surface area, they represent proportionally high C fluxes. For example, Holgerson and Raymond (2016) estimated the global CO_2 and diffusive CH_4 fluxes from lakes and ponds according to their size distribution (Table 1.1) and they

found that small lentic waterbodies emit high rates of GHG to the atmosphere across their collective surface area. More specifically, small lakes and ponds < 0.001 km^2 are estimated to represent 15.1% and 40.6% of global CO_2 and CH_4 lentic emissions, even if they comprise only 8.6% of estimated global lakes and ponds area (Holgerson & Raymond, 2016), due to higher areal emissions as exemplified in 68 globally distributed ponds and wetlands (Holgerson et al. 2017). In particular, Figure 1.1 shows that small waterbodies have areal emissions several times (up to 10x) higher than for larger systems for both CO_2 and CH_4, and that areal rates of emissions tend to go down with area.

Table 1.1 Global carbon emissions from lakes and ponds (Holgerson and Raymond, 2016).

Size Class (km^2)	Surface Area		CO_2 flux			Diffusive CH_4 flux		
	km^2	%	$PgCy^{-1}$	$mgCm^{-2}d^{-1}$	%	$PgCy^{-1}$	$mgCm^{-2}d^{-1}$	%
<0.001	147,763 – 861,578	8.6	0.0890	966.5	15.1	0.00643	69.8	40.6
0.001-0.01	406,576	6.8	0.0425	286.4	7.4	0.00125	8.4	10.4
0.01-0.1	675,234	11.3	0.0689	279.5	12.0	0.00101	4.1	8.4
0.1-1	984,651	16.5	0.1215	338.1	21.3	0.00102	2.8	8.5
1-10	782,074	13.1	0.0802	280.9	14.0	0.00079	2.7	6.6
10-100	597,789	10.0	0.0537	246.1	9.4	0.00037	1.7	3.1
>100	2,024,016	34.0	0.1152	155.9	20.2	0.00067	0.9	5.6
Total	5,618,103 - 6,331,918		0.571			0.012		

It is predicted that the intensity of CO_2 evasion from small streams and rivers across their collective surface area is high (Raymond et al., 2013), like small ponds and lakes (Downing et al., 2012). The estimated ice-free global active inland lotic surface area is 0.54 million km^2 and evades 1.8 $PgCO_2y^{-1}$ (Raymond et al., 2013). The estimated global flux of diffusive CH_4 is 26.8 Tgy^{-1} using a bootstrapping approach by multiplying the estimated flowing surface area (Stanley et al., 2016). Therefore, the relationship between aquatic ecosystems area and areal rates of GHG emissions appear to hold for lakes, ponds, and rivers, because small waterbodies have higher connectivity with land and sediments.

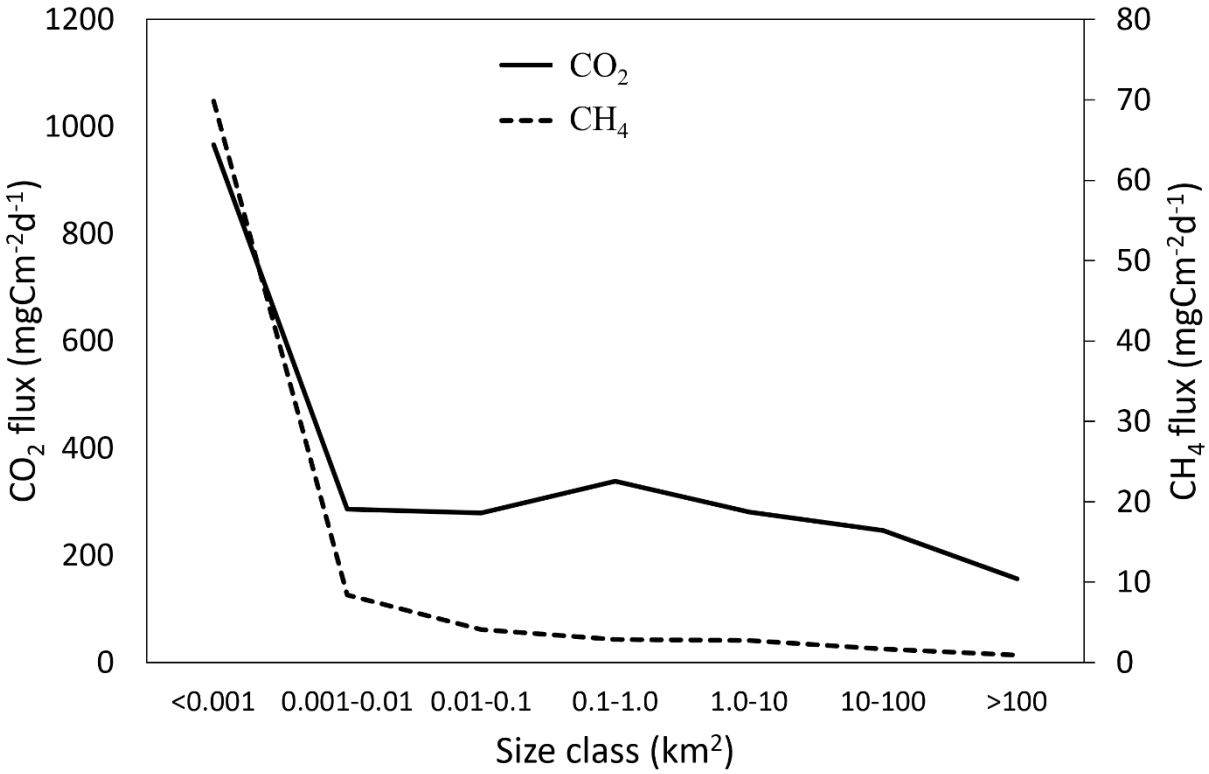

Figure 1.1 Global CO_2 and CH_4 fluxes from lakes and ponds according to their size distribution. Data plotted from Holgerson and Raymond 2016.

1.3 Global abundance and size distribution of small waterbodies

It is important to know the global abundance and size distribution of lotic and lentic inland surface water systems in order to properly estimate and integrate their role and contribution to the global C cycle and other biogeochemical processes. Few studies have been done to estimate the global riverine area (e.g., Lehner & Döll, 2004; Downing, 2009; Aufdenkampe et al., 2011), but the small stream orders were overlooked in these estimations. By analyzing aerial satellite images, Lehner and Döll (2004) estimated the global river and stream areas of 0.36 million km^2 ($\geq$0.1 km^2) which covers 0.3% land surface area. But, Downing et al. (2012) estimated 0.48 million km^2 global fluvial area that covers approximately 0.56% of the global land area excluding ephemeral streams fraction (Table 1.2). Almost 35% of the global riverine area (stream orders 1 to 5) were overlooked in the back-estimate by Lehner and Döll (2004). Despite comprising only 17% of the estimated

global fluvial surface area, the abundance of small streams (orders 1-3) is higher (almost 29.8 million) compared to larger lotic waterbodies (Downing et al., 2012; Table 1.2).

Table 1.2 Stream order, size, number and area of global stream and river (Downing et al., 2012).

Stream Order	Number	Mean length (km)	Mean Width (m)	Mean Area (km^2)	Total Area	
					km^2	%
1	28,550,000	1.6	0.8	0.001	36,500	5.5
2	6,000,000	3.7	1.8	0.007	39,200	5.9
3	1,260,000	8.5	3.7	0.03	39,600	6.0
4	264,000	19.5	8.3	0.16	42,500	6.4
5	55,500	44.8	29.3	1.31	72,800	11.0
6	11,700	103.2	73.3	7.56	88,100	13.3
7	2,450	237.4	131.5	31.22	76,400	11.5
8	515	546.2	264.5	144.47	74,300	11.2
9	110	1256.7	608.5	764.70	82,600	12.5
10	23	2891.7	988.5	2,858.44	64,900	9.8
11	5	6653.8	803.0	5,343.00	25,400	3.8
12	1	6437.0	3079.0	19,800.00	19,800	3.0
Total	36,144,304				662,100	

A few studies on the global size distribution and abundance of lakes have been done by statistical extrapolations (Downing et al., 2006) and map compilations analysis (Lehner & Döll, 2004; Verpoorter et al., 2014). Lehner and Döll (2004) computed the total global lake area of 2.4 million km^2 which occupies 1.8% of continental land area, but they only considered lakes larger than 0.1 km^2 in this calculation. Downing et al. (2006) estimated the global lake area of 4.2 million km^2 after including the lake size less than 0.1 km^2 for the first time in their statistical extrapolation calculation. They found that Lehner and Döll (2004) omitted 301 million small lakes and 30.8% lake area in the size range of 0.001 to 0.1 km^2 in their calculation (Table 1.3). But recently it has been found that the statistical extrapolation analysis using Pareto distribution inappropriately computes the abundance of small lakes (Seekell & Pace, 2011; McDonald et al., 2012). Map compilation analysis using high-resolution satellite imagery is an accurate way to estimate the global abundance and size distribution of lakes (Seekell & Pace, 2011; Verpoorter et al., 2014). Verpoorter et al. (2014) computed 5.4 million km^2 global lake surface area using high-resolution

satellite imagery analysis that covers 3.6% of Earth's land surface and includes a total of 117 million lakes. Accordingly, there are about 113 million small lakes and ponds in the size range of 0.002 to 0.1 km^2 and they occupy only 19% of the total global lake area (Table 1.3). Recently, Messager et al. (2016) estimated 2.67 million km^2 global surface lake area which cover 1.8% global land area using geo-statistical model (Table 1.3), but they only considered lakes larger than 0.1 km^2. Moreover, Feng et al. (2016) computed total global inland surface water bodies (i.e., lakes, rivers and reservoirs) of 3.65 million km^2 using 30-m high-resolution dataset. So, Verpoorter et al. (2014) may have over-estimated lake number area by overlapping with wetlands, reservoirs, and rivers due to misclassification of open water features by remote sensing-based map compilation estimate (Messager et al., 2016; Feng et al., 2016). Overall, small lotic and lentic waterbodies tend to be more abundant in terms of numbers (Table 1.2, 1.3), areal rates of fluxes (Table 1.1), although they do not represent the majority of the global surface.

1.4 Peatland: heterogeneity of C dynamics

1.4.1 Peatlands: net C sink

A major, but poorly characterized portion of the world's small waterbodies consists of peatland pools, which are found in peat ecosystems that can dominate the landscape in certain areas. Peatlands are heterogeneous C-rich wetland ecosystems characterized by the natural accumulation of partially decomposed decaying vegetation-derived organic matter (OM) referred to as peat in permanent low oxygenic waterlogged environment (Finlayson & Milton, 2018). Despite occupying only 2.8% of the world's land area (Xu et al., 2018), they contain almost 30% (Table 1.4) of total soil C stock (1500 Pg C) in the biosphere (Yu et al., 2010). They are net C accumulators because the net primary production (NPP) of vegetation is higher than peat decomposition (Waddington & Roulet, 2000) due to oxygen-depleted waterlogged conditions which slows the decomposition processes to such an extent that vegetation-derived OM stores as peat (Figure 1.2). Despite being a large C repository, CH_4 is produced in water-logged anoxic peat as a function of decomposition through acetoclastic methanogenesis using acetate as an electron acceptor as well as hydrogenotrophic methanogenesis which reduces CO_2 to CH_4 using hydrogen (H_2) as an electron donor (Schlesinger & Bernhardt, 2013). Hydrogenotrophic methanogenesis tends to be the dominant CH_4 production pathway in bogs, whereas acetoclastic methanogenesis is

typically dominant pathway in fens (Bridgham et al., 2013). Moreover, CO_2 is also produced from autotrophic respiration of root carbohydrates and exudates, aerobic respiration of heterotrophic microbes, and oxidation of peat-produced CH_4 (Sayer & Tanner, 2010). This peat-produced GHG is released to the atmosphere through diffusion, ebullition, and vegetation-mediated transport (Pelletier et al., 2014).

DOM serves different chemical and ecological functions in peatlands (Moore, 2009) and controls the balance between carbon accumulation from the soil OM decomposition, vegetation litter leaching and root exudates, and carbon loss as GHG emission and surface runoff (Pinsonneault et al., 2016). It is the key vital component of carbon dynamics in peatland ecosystem (Moore et al., 2011), although DOM dynamics in peat porewater is poorly known. In peat porewater, DOM serves as energy of microorganisms, produces GHG, and controls acidification and nutrients speciation (Limpens et al., 2008). DOM in oxygen-depleted water-logged peat may degrade through methanogenesis and/or microbial decomposition and produced CH_4 and CO_2 (Chanton et al., 2008). DOM composition can reveal the carbon dynamics in peatland ecosystem by reflecting its origin (vegetation derived, microbial production, peat leaching) (Fellman et al., 2008).

Peatland ecosystems are diverse in terms of shape, size, vegetation cover and spatial distribution due to their geomorphology and climatic condition (Finlayson & Milton, 2018; Xu et al., 2018; Page et al., 2011). Peatlands are classified into two main types based on their water and nutrients sources: minerotrophic (fens) and ombrotrophic (bogs). Fens are mainly reliant on groundwater or surface water flows for their water and nutrients (Lindsay, 2016). In contrast, bogs are hydrologically disconnected from the surrounding uplands and receive their water and nutrients entirely from precipitation (Lindsay, 2016). Bogs are generally characterized by water-saturated high acidic organic soils and low nutrients availability with similar biogeochemical functions, floristic compositions, and hydrological settings. Water table lowering and higher evapotranspiration than precipitation can convert the peatlands into net sources of atmospheric GHG (Holden, 2006).

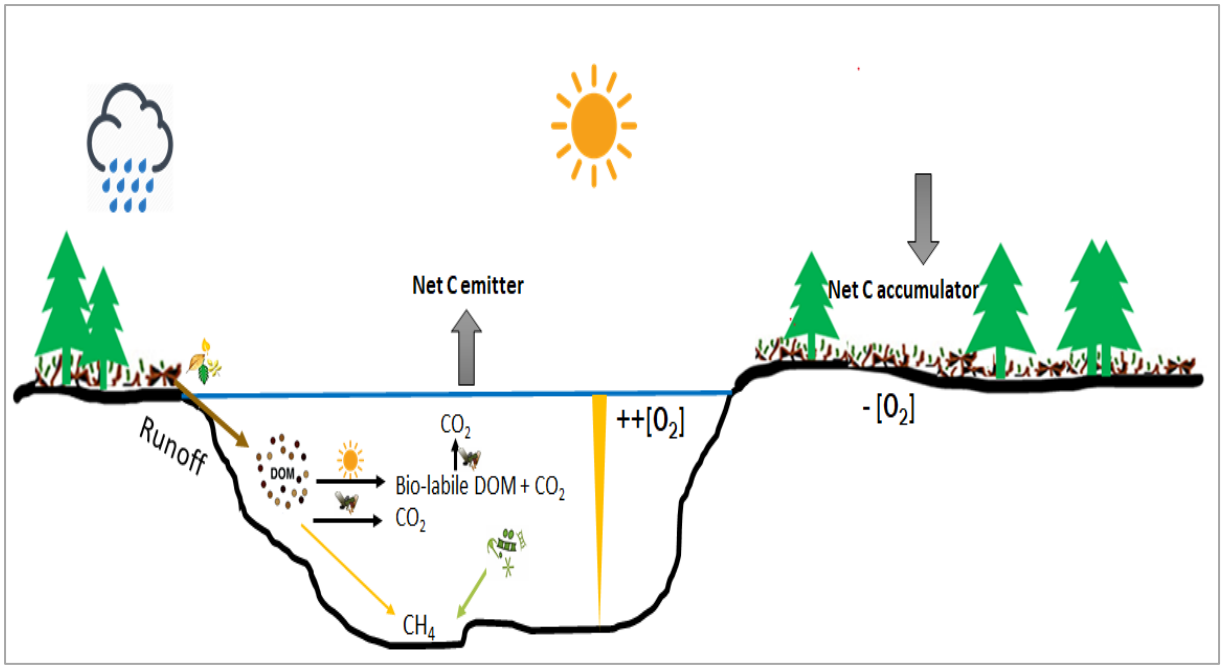

Figure 1.2 Terrestrial parts of peatlands are net carbon accumulators whereas aquatic parts are net carbon sources to the atmosphere. High rates of vegetation net primary production (NPP) compared to peat decomposition in waterlogged oxygen-depleted terrestrial parts of peatland ecosystems. Photochemical and biological degradation in aquatic parts produce and emit more carbon compared to carbon uptake by the limited aquatic vegetation.

Table 1.3 Size, number, and area of world lakes and ponds.

Statistical extrapolation estimate (Downing et al., 2006)				Remote sensing-based map compilation estimate (Verpoorter et al., 2014)				Geo-statistical model estimate (Messager et al., 2016)		
Size class (km^2)	Number of Lakes	Total area of lakes		Size class (km^2)	Number of Lakes	Total area of lakes		Size class (km^2)	Number of Lakes	Total area of lakes (km^2)
		km^2	%			km^2	%			
0.001-0.01	277,400,000	692,600	16.5	0.002-0.01	90,000,000	364,864	6.6			
0.01-0.1	24,120,000	602,100	14.3	0.01-0.1	23,725,071	683,000	12.4			
0.1-1	2,097,000	523,400	12.5	0.1-1	3,813,612	995,000	18.1	0.1-1	1,241,200	348,400
1-10	182,300	455,100	10.8	1-10	331,452	793,000	14.4	1-10	165,100	411,000
10-100	15,905	392,362	9.3	10-100	24,332	611,000	11.1	10-100	13,400	331,600
100-1,000	1,330	329,816	7.8	100-1,000	1,948	489,000	8.9	100-1,000	1,220	313,500
1,000-10,000	105	257,856	6.1	1,000-10,000	211	537,000	9.8	1,000-10,000	115	313,300
10000-100,000	16	607,650	14.5	>10,000	20	1,020,000	18.5	>10,000	18	959,100
>100,000	1	378,119	9.0							
All lake	304,000,000	4,200,000			117,896,646	5,494,864			1,421,053	2,676,900

Table 1.4 Global distribution of peatlands and their storage carbon (Yu et al., 2010).

Regions	Land area		Average carbon storage	
	km^2	%	GtC	%
Northern peatland	4,000,000	90.7	547	89.4
Tropical peatland	368,500	8.3	50	8.2
Southern peatland	45,000	1.0	15	2.4

1.4.2 Peatland ponds: net C source

Peatland ponds are common autogenic microform features in both the Northern and Southern hemispheres (Glaser, 1999) that may play a vital role in the C dynamics of peatlands (Waddington & Roulet, 2000). Peatlands are important global C sinks due to their higher rate of net primary production (NPP) of the peatland vegetation than peat decomposition throughout the millennia (Waddington & Roulet, 2000; Frolking et al., 2001). However, the aquatic processes in peatland ponds may reverse this role as opposed to their vegetated areas because they are generally considered net C sources to the atmosphere (Waddington & Roulet, 2000; Repo et al., 2007; McEnroe et al., 2009; Pelletier et al., 2014). Carbon emissions from ponds may be due to bottom peat decomposition, photo- and microbial degradation of DOM as well as low atmospheric C uptake by the limited aquatic vegetation (Pelletier et al., 2014). The contribution of ponds to ecosystem C emissions is typically overlooked although they occupy a significant area of some peatland ecosystems. For example, peatland ponds cover more than 40% area of some peatland ecosystems in the Hudson Bay Lowlands (Roulet et al., 1994). Peatland waterbodies (i.e., peatland ponds and lakes) occupy almost 0.26 million km^2 surface area in the northern hemisphere (Olefeldt et al., 2021). There is thus a need to better understand C dynamics in peatland ponds given their role in the global C cycle. Ombrotrophic peatland ponds were considered in this study because they are abundant, but their biogeochemistry as well as bog groundwater is not influenced by surrounding mineral areas, hence they likely behave differently compared to more broadly studied lentic ecosystems. Therefore, this study will give us the insight mechanisms of C dynamics in bog pools and their role in the peatland C cycle as well as the global C cycle.

1.5 External and internal factors controlling C dynamics in ponds

There is very little information on C cycling in peatland ponds compared to other types of ponds and small lakes. Climate change and landscape position significantly influence the floristic composition and peat characteristics as well as morphometry of peatlands, which all directly or indirectly influence the C dynamics in peatland ponds (Figure 1.3). Landscape position influences vegetation composition (Bengtsson et al., 2020) by controlling the precipitation chemistry and atmospheric deposition of nutrients (especially N) **(**Haragushi et al., 2003). Small N deposition in N-limited sites stimulates sphagnum moss growth, but higher deposition of N depresses growth (Lampen et al., 2011). Higher N deposition promotes higher plant growth that reduces light

availability and surface temperature and increases litter that in turn depresses sphagnum mosses growth (Chong et al., 2012). The abundance of vascular plants increases with an increased temperature, precipitation, N deposition, and deeper water table (Bengtsson et al., 2020). Peat-forming organic matter (OM) originated from different types of vegetation may show distinct characteristics which result in different decomposition rates of OM and GHG production (Hoyos-Santillan et al., 2015).

Morphometry strongly influences the C dynamics in peatland pools. For example, McEnroe et al. (2009), Turner et al. (2016) and Arsenault et al. (2018) found GHG emission and concentration inversely related with pool area and depth. This was attributed to increasing decomposition activities in small shallow ponds due to high terrestrial C loading, temperature and DO (McEnroe et al., 2009). Moreover, morphological characteristics of pools (shallow and small size) favor energy penetration and warming of organic-rich sediment (Wik et al., 2014) which increase bacterial activity and bottom peat decomposition (Pelletier et al., 2014).

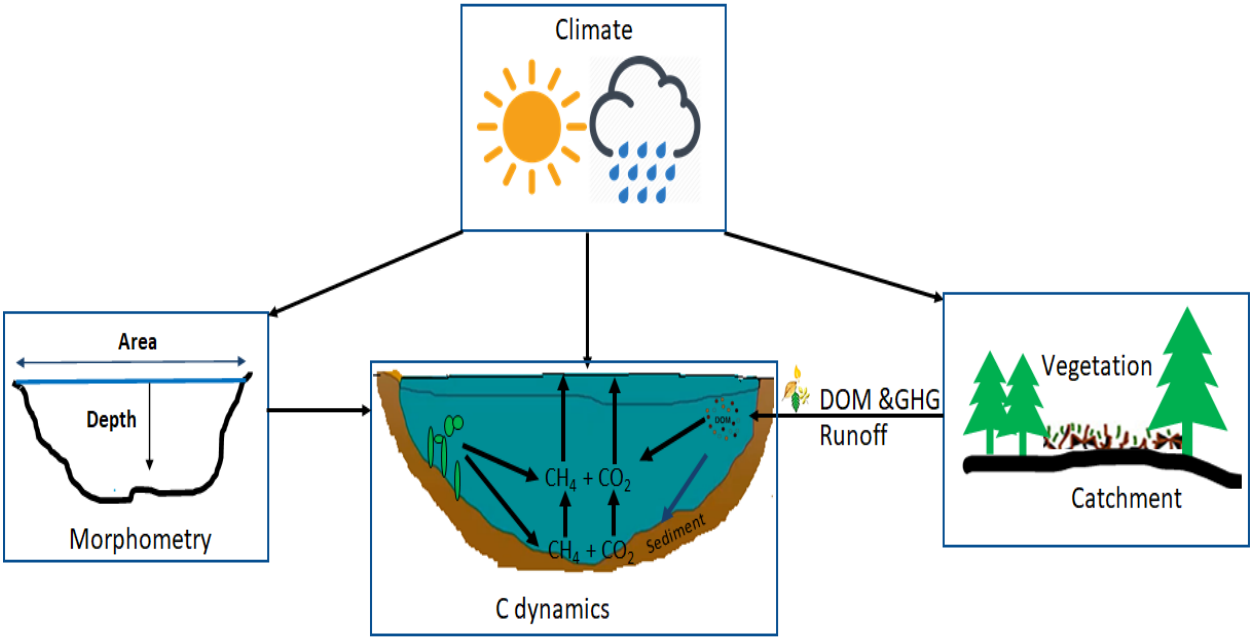

Figure 1.3 External and internal factors control carbon dynamics in small lentic waterbodies.

Aquatic processes (photochemical and microbial degradation) and water chemistry may influence the in-situ C dynamics in peatland ponds. The major source of CO_2 production in lentic system is most likely the mineralization of allochthonous OM (Sobek et al., 2003), an important driver of heterotrophic metabolism in lakes (Algesten et al., 2005). Photo-mineralization, an important natural phenomenon of GHG production, is photo-oxidation of allochthonous DOM to CO_2 by solar radiation (Li et al., 2019). Solar radiation can also transform recalcitrant DOM to bio-labile DOM molecules which accelerate the microbial respiration (Jonsson et al., 2001). But the actual role of photo-mineralization, considering the frequent mixing of water in high terrigenous DOC loading lentic small waterbodies, is unknown. Methanogenic CH_4 production in anoxic lake and pond sediments is mainly influenced by the temperature through stimulating microbial activity and availability of terrestrial loaded or in-situ produced labile OM for decomposition (Yvon-Durocher et al., 2014). For example, high autochthonous OM in pond sediment is associated with elevated CH_4 concentration (Webb et al., 2019). The nutrient content stimulates the microbial activities both in oxic and anoxic environment (Peacock et al., 2019; Webb et al., 2019), potentially leading to high CO_2 and CH_4 production. Small waterbodies have a higher sediment area to water volume ratio than larger waterbodies and less possibility of CH_4 oxidation in the water column due to low depth (Juutinen et al., 2009). Therefore, C fluxes in small waterbodies may depend on the climate, hydrological settings and, landscape properties and position as well as internal biogeochemical characteristics.

1.6 The role of DOM for C cycling in small waterbodies

DOM is an important intermediate in the global C dynamics as it acts as a major source for GHG production as a function of photochemical and biological degradation. DOM controls the structure of communities and ecosystems as a vector of energy and nutrients from terrestrial to aquatic environment (Jansson et al., 2007). But there is little information on DOM patterns in peatland pools and their impact on GHG dynamics. Studies from other types of ecosystems suggest that terrestrial DOM can be labile for both biodegradation and photodegradation. For example, 70-95% DOM was degraded through photodegradation in Arctic lakes and rivers (Cory et al., 2014), although all freshwater environments do not show the same type of DOM processing. D'Amario and Xenopoulos (2015) found that high molecular weight, aromatic and larger allochthonous DOM composition is an important predictor of CO_2 concentrations in streams. The reason why DOM

composition may be an important explanatory variable of CO_2 is that complex and larger DOM is more photo-sensitive compared to smaller DOM and is more respired by microbes than assimilated (Fellman et al., 2009). As well, studies showed that lignin-derived DOM compounds from vascular plants were highly resistant to biological mineralization, but polyphenols and polycondensed aromatics from plants are more reactive to photo-mineralization (Mostovaya et al., 2017). Another mechanism to support this point is the larger DOM compounds photodegraded into more bio-labile smaller and simple DOM fractions and CO_2 (Figure 1.4a) (Lou & Xie, 2006). Elevated terrestrial humic-rich DOM enhances CH_4 concentration in eutrophic lakes (Zhou et al., 2018). The mechanism to support this statement is solar radiation at higher UV and PAR (photosynthetic active radiation) light ranges can lead to photodegradation of terrestrial derived DOM into bio-labile DOM fractions with dissolved CH_4 production in dissolved oxygen (DO) depleted aquatic environment (Figure 1.4b) (Bange & Uher, 2005; Cory et al., 2014). On the other hand, autochthonous algal-derived DOM has been associated with high CH_4 production in aquatic environments (Webb et al., 2019) which can be linked to high primary production at the bottom or in the water column, leading to partial anoxia in certain zones (Bogard et al., 2014). Therefore, there are different pathways that could link DOM composition and GHG concentrations in peatland pools, hence a better understanding of how DOM composition may be linked to GHG patterns can help understand spatial and temporal patterns in C cycle of this organic-rich aquatic systems.

1.7 Research questions

DOM is an important intermediate in wetland carbon dynamics but its actual role in GHG production remains unexplored in peatland pools. To date, several studies have been done concerning C emission (especially CH_4) from the terrestrial part of peatlands, whereas very few studies have been done on the aquatic parts and mostly focused on greenhouse gas (GHG) fluxes. But the patterns of GHG production and their driving factors in the peatland pools are mostly unknown on a small as well as a broader scale. Therefore, there is a need to better understand the spatial intra- and inter-regional patterns of CO_2 and CH_4 levels in peatland pools and their drivers.

In this context, this project was focused on the following three research questions to fill the key knowledge gaps that have been identified. This research was carried out using the

ombrotrophic peatland pools' data which were measured from Québec (Canada) and Chilean Patagonia (Figure 1.5).

Q1- ***How do climate (i.e., temperature and precipitation), vegetation cover, morphometry (i.e., depth and surface area) and water chemistry of ombrotrophic bog pools affect intra- and inter-regional spatial patterns of DOM composition and concentration as well as dissolved CO_2 and CH_4 concentrations?***

Q2-Which drivers are responsible for the temporal variation of DOM compositions and concentrations as well as dissolved GHG concentrations?

Q3- What is the relation between DOM composition and dissolved greenhouse gas (CO_2 and CH_4) concentrations?

These questions are answered in the next chapter, which corresponds to the manuscript of a scientific article.

(a)

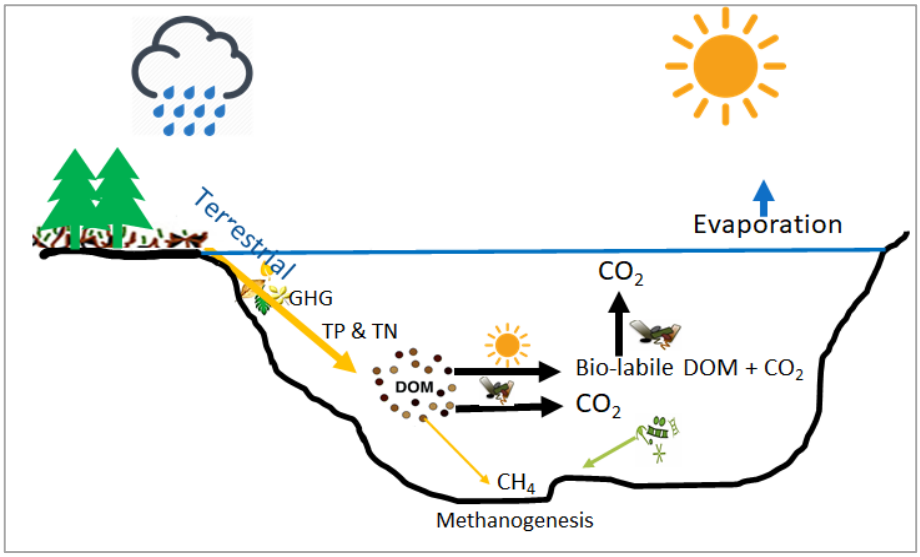

(b)

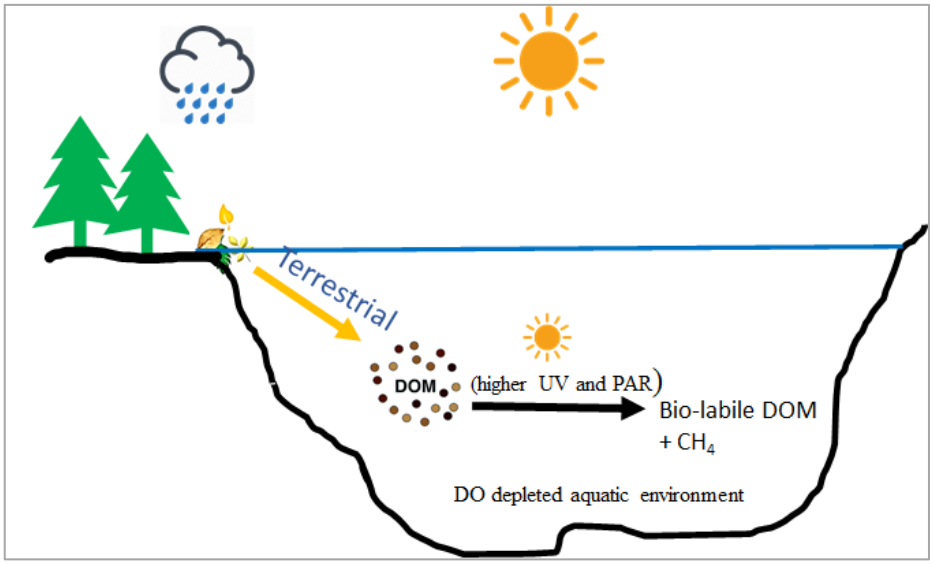

Figure 1.4 Carbon dynamics in aquatic systems. (a) Mechanism of CO_2 production through photochemical and biological degradation in oxic environment as well as CH_4 production in anoxic environment through methanogenesis. (b) Mechanism of CH_4 production in water column through photochemical degradation of terrestrial derived DOM in a low oxygen-depleted environment.

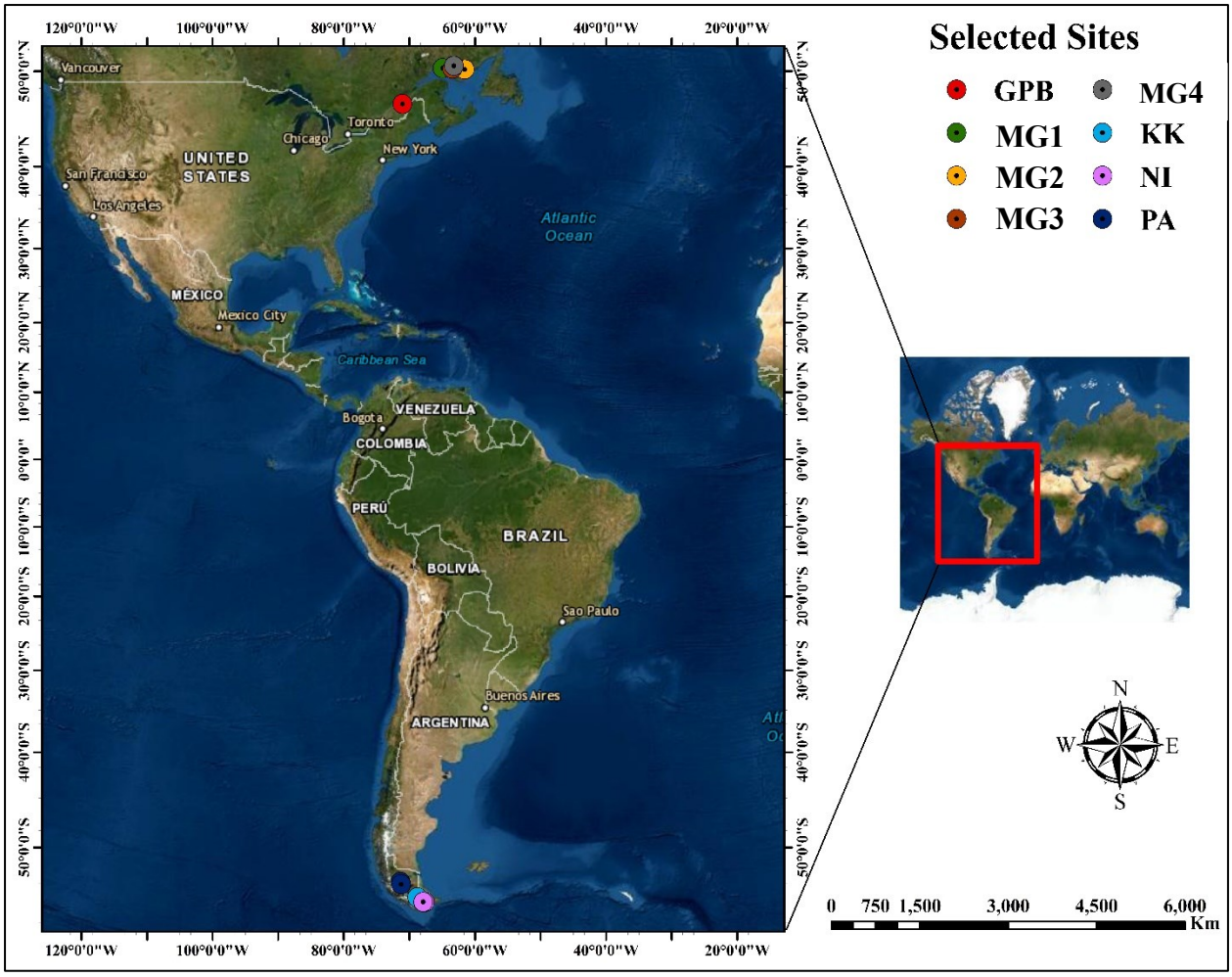

Figure 1.5 Map of the study area. The study sites are in the Grande plée Bleue (GPB; southern Québec), the Minganie region (MG; eastern Québec), Canada, and three Chilean Patagonian regions named Punta Arenas (PA), Karukinka (KK), and Navarino Island (NI).

Chapter 2: Linking Dissolved Organic Matter to CO_2 and CH_4 Concentrations in Canadian and Chilean Peatland Pools

Contribution of the authors

Hassan, M., Talbot, T., Arsenault, J., Martinez-Cruz, K., Sepulveda-Jauregui, A., Hoyos-Santillan, J. and Lapierre, J-F. Linking Dissolved Organic Matter to CO_2 and CH_4 Concentrations in Canadian and Chilean Ombrotrophic Bog Pools. *Global Biogeochemical Cycles*, article in under review.

Chapter 2 is presented as a research article which is in under review for publication. Authors contributions are listed below:

- Hassan, M.: Project design, sample analysis, data processing, initial and final drafting
- Talbot, T.: Project design, laboratory and field logistics, field work, final drafting, co-supervision
- Arsenault, J.: Project design, sample analysis, field work, revision of the final version
- Martinez-Cruz, K.: Contribution in Chilean sampling, revision of the final version
- Sepulveda-Jauregui, A.: Contribution in Chilean sampling, revision of the final version
- Hoyos-Santillan, J.: Contribution in Chilean sampling, revision of the final version
- Lapierre, J-F.: Project design, Study framing, supervision of DOM analyses, final drafting, supervision

Linking Dissolved Organic Matter to CO_2 and CH_4 Concentrations in Canadian and Chilean Peatland Pools

Mahmud Hassan[1], Julie Talbot[2], Julien Arsenault[2], Karla Martinez-Cruz[3,4], Armando Sepulveda-Jauregui[3], Jorge Hoyos-Santillan[3,5], and Jean-François Lapierre[1]

[1]Département de sciences biologiques, Université de Montréal, Montreal, Québec, Canada
[2]Département de Géographie, Université de Montréal, Montreal, Québec, Canada
[3]Environmental Biogeochemistry Laboratory (EBL), University of Magallanes, Punta Arenas, Chile
[4]Environmental Physics, Limnological Institute, Universität Konstanz, Konstanz, Germany
[5]School of Biosciences, University of Nottingham, Sutton Bonington, Loughborough, UK

Key points:

- Broad-scale patterns in climate, vegetation cover and pool morphometry control cross-regional patterns in dissolved organic matter (DOM) and greenhouse gases (GHG), and their links
- DOM and GHG relate non-linearly with long-term temperature and precipitation patterns across regions
- Protein-like DOM controls within pool GHG concentrations across regions, while humic-like DOM drives within-site temporal GHG concentrations

2.1 Abstract

Peatland open-water pools can be net carbon (C) emitters within heterogeneous peatland ecosystems that are generally net C sinks. However, the intra- and inter-regional patterns and drivers of greenhouse gas (GHG) production, as well as their link with dissolved organic matter (DOM) quality and quantity, remain poorly understood. We analyzed a range of optical and chemical variables controlling DOM and GHG concentrations in 73 peatland pools across five regions with changing geographic properties (*i.e.*, climate, topography, morphometry, and vegetation cover) of eastern Canada and Chilean Patagonia. We found inter-regional patterns in GHG and DOM concentrations and composition that were coherent with patterns in mean annual temperature and precipitation, and vegetation cover. Inter-regional patterns of GHG were driven by morphometry, vegetation cover, and protein-like DOM composition whereas temporal variations of GHG were further influenced by seasonal changes in humic-like DOM composition, dissolved organic carbon (DOC) and nutrients (*i.e.*, TP and TN) concentrations, as well as pH and oxygen levels. Our results show that inter-regional C-cycling in peatland pools is primarily driven by broad-scale geophysical constraints, whereas seasonal patterns at the intra-regional scale are primarily driven by local-scale drivers that dictate highly variable water chemistry and internal processes. This study suggest that geophysical constraints may change the net role of peatlands as an accumulator by influencing the C dynamics in pools, highlighting the importance of peatland pools in peatland ecosystems, as well as in the global C cycle under rapid environmental changes.

Keywords: Peatland pools, climate, vegetation cover, morphometry, dissolved organic matter, greenhouse gases.

2.2 Introduction

Peatlands are an important global carbon (C) sink as net primary production (NPP) is higher than peat decomposition over millennial time scales (Waddington & Roulet, 2000; Frolking et al., 2001). Nevertheless, peatland open-water pools play a particular role in the C dynamics of heterogeneous C-rich peatland ecosystems, as they are often net C sources to the atmosphere (Waddington & Roulet, 2000; Repo et al., 2007; McEnroe et al., 2009; Pelletier et al., 2014; Turner et al., 2016). This can be due to peat decomposition at the bottom of pools, photochemical and microbial degradation of dissolved organic matter (DOM), as well as low atmospheric C uptake by the limited aquatic vegetation (Pelletier et al., 2014). Decomposition at the bottom of peatland pools is higher than in other freshwater systems due to morphological characteristics of pools (small and shallow) that enhance the direct uptake of energy from the environment (Wik et al., 2014, 2016). The heterogeneity of C accumulation and emission between terrestrial and aquatic parts of peatlands has seldom been included in the contemporary C budget for these ecosystems (Pelletier et al., 2015). There is limited information on the patterns and drivers of C cycling within peatland pools compared to their vegetated areas as well as other small freshwater ecosystems.

Multiple properties (*i.e.*, climate, hydrology, morphology, vegetation cover, and water chemistry) dictate the spatial and temporal patterns in the C cycling of small lakes, ponds and wetlands (Kuhn et al., 2021; Arsenault et al., 2018; Turner et al., 2016; Wik et al., 2016; DelSontro et al., 2016; Holgerson et al., 2015). Yet, it is unclear how these processes drive C cycling in peatland pools (Arsenault et al., 2022). In small waterbodies, climate (*i.e.*, temperature and precipitation) and hydrological connectivity influence the production of greenhouse gases (GHG) by affecting internal biogeochemical processes (*i.e.*, photo-chemical and microbial degradation, primary production, and water chemistry) (Zhong et al., 2020; Serikova et al., 2019; Wik et al., 2016; Weyhenmeyer et al., 2015). For example, warming temperatures increase methane (CH_4) production in ponds and small peatland lakes during summer by stimulating methanogenic activity in sediments (Holgerson, 2015; Kuhn et al., 2021). Temperature also increases the activities of heterotrophic microbial respiration and hence increases carbon dioxide (CO_2) production in water columns and sediments (Kosten et al., 2010; Sobek et al., 2017; Yvon-Durocher et al., 2014). Depending on catchment characteristics (*e.g.*, vegetation cover, soil characteristics,

geomorphology), increased precipitation can lead to elevate concentrations of CO_2 (Roehm et al., 2009; Einola et al., 2011) and CH_4 (Natchimuthu et al., 2014) through the input of terrigenous dissolved organic carbon (DOC) to small waterbodies. On the contrary, precipitation and CH_4 concentrations can be inversely related due to the dilution of DOM and nutrients and an increase in dissolved oxygen in small ponds after precipitation events (Holgerson et al., 2015). Groundwater flow can transport terrestrial DOM and nutrients from peat to pools during wet periods when peat has higher water levels than pools, creating a positive hydrological gradient from the peat to the pool (Arsenault et al., 2019). Lateral exchanges with the surrounding peat may also transport CO_2 and CH_4 produced in the organic soil (*e.g.*, Weyhenmeyer et al., 2015; Cobb et al., 2017). Peatland pools are generally nutrient poor and nutrients typically do not show significant influence on CO_2 and CH_4 production (Turner et al., 2016).

DOM is an important player in the global C cycle as it acts as an indirect modulator of multiple aquatic biogeochemical processes (Prairie, 2008), including the availability of substrates for CO_2 and CH_4 production (Coble, 2007). In peatland pools, DOM quality is influenced by the peat characteristics and vegetation cover. For example, Arsenault et al. (2018) found higher specific UV absorbance (SUVA), which indicating more aromatic and recalcitrant DOM, in pools surrounded by trees and shrubs than those surrounded by mosses. SUVA and CO_2 concentration were positively correlated in artificial urban ponds (Peacock et al., 2019) and peatland pools (Arsenault et al., 2018; Turner et al., 2016; Pelletier et al., 2014). As for morphology, pool surface area and depth have a significant inverse relationship with CO_2 and CH_4 fluxes (McEnroe et al., 2009). Together, this suggests that spatial and temporal patterns in climate, peat characteristics, and water environmental properties may lead to predictable patterns in DOM quality and quantity as well as GHG concentrations in peatland pools, but there is a lack of empirical data supporting this hypothesis.

Long-term averages of climate (*e.g.*, mean annual temperature or precipitation) have been shown to correlate with broad-scale patterns in aquatic ecosystems, because such measurements are highly structured in space (Lapierre et al., 2018). Most climate variables used to predict aquatic ecosystem functioning, however, have relatively low temporal (yearly to decadal scales) compared to spatial variation (Soranno et al., 2020). Given their impact on aquatic C cycling, climatic

conditions may thus induce broad-scale patterns in the C biogeochemistry of peatland pools but not lead to strong intra-regional or temporal patterns. Cross-regional variability of peatland pool DOC and GHG concentrations as well as other water chemistry is higher than within-regions due to variability in geophysical properties (Turner et al., 2016). Landscape position (*e.g.*, distance from the sea) affects the internal biogeochemical characteristics of peatland pools (Turner et al., 2016) and freshwater wetland ponds (Vizza et al., 2017) by influencing the precipitation chemistry, and by enhancing the atmospheric deposition of sea-borne cations (Haragushi et al., 2003). The small scale intra-regional studies in ponds and peatland pools have thus found that more local drivers (*e.g.*, pond depth and area) influence the production and distribution of GHG concentrations, while climate and topography may explain broader scale patterns in peatland pools C cycle, but this has rarely, if ever, been tested in a single study.

In this context, our goal was to assess and quantify patterns and drivers of DOM and dissolved CO_2 and CH_4 in peatland pools with changing geographic properties. We did so by collecting data from eight peatland sites located across five regions of eastern Canada and Chilean Patagonia. Our specific objectives were to: (1) determine the influence of intra- and inter-regional patterns of climate, topography, morphology, vegetation cover and water environmental properties on DOM composition and GHG concentrations in peatland pools, 2) evaluate the temporal variability of climatic conditions and water environmental properties, and subsequent impacts on DOM composition and GHG concentrations within a region, and (3) assess the effects of DOM composition on GHG concentrations.

2.3 Methodology

2.3.1 Site description

Our study sites comprise natural, undisturbed ombrotrophic and blanket (formed in ombrotrophic settings) bogs located in the Québec City (southern Québec) and the Minganie regions (eastern Québec), Canada, and in the Punta Arenas City (continental Magallanes), the Karukinka Park (Tierra del Fuego Island), and Navarino Island (Cape Horn) regions, Chile. The ombrotrophic bogs are hydrologically disconnected from the surrounding uplands and receive their water and nutrients from atmospheric deposition.

In southern Québec, we sampled the Grande plée Bleue (GPB) peatland, which is undisturbed. GPB is located 12 km southeast of Québec City and has an area of 15 km^2 (46°47′N, 71°03′W). The hydrologically isolated ombrotrophic conditions of this peatland have existed for 8300 years but peat accumulation began around 9500 cal. y BP (calibrated years before present) over the Goldthwait Sea sediments (Lavoie et al., 2012). This peatland is located in the cool continental climate region with a mean annual temperature (MAT) and precipitation (MAP) of 3.9 °C and 1329 mm (Table 2.1), respectively (data obtained from the 1991 to 2020 Climatic Research Unit gridded Time Series dataset (CRU TS v.4.05)). The dominant vegetation species in the peatland are *Sphagnum* mosses (*e.g.*, *Sphagnum fuscum, S. medium* and *S. angustifolium*) except for some areas that are dominated by sparse shrubs (*e.g.*, *Kalmia angustifolia* and *Chamaedaphne calyculata*) or graminoids (*e.g.*, *Carex spp., Eriophorum virginicum*, and *Rhyncospora spp.*). A central forested part is dominated by trees (*e.g.*, *Picea mariana* and *Larix laricina*).

In eastern Québec, we sampled four peatlands in the Minganie (MG) region (50°19′N, 63°17′W) which were located along a ~250 km east-west transect in the maritime boreal and subarctic ecotone along the Gulf of St-Lawrence. MAT (1.0 °C) and MAP (962 mm) (Table 2.1) of MG sites are lower than that of St-Lawrence lowlands (Climate normal 1991-2020; CRU TS v.4.05). The peatlands of MG are mostly covered by mosses (*e.g.*, *Sphagnum capillifolium*, *S. fuscum*, and *S. medium*, ericaceous shrubs (*e.g.*, *Kalmia angustifolia, Chamaedaphne calyculata,* and *Betula pumila*), herbaceous plants (*e.g.*, *Nuphar variegate. Trichophorum cespitosum, graminoids*), and lichens. These peatlands are mostly treeless except for interspersed *Larix laricina* and *Picea mariana*.

Patagonian peatlands developed during the last post-glaciation in the range of 9000-12000 cal. y BP (early Holocene) and are latitudinally distributed along about 2000 km across two countries (Southern Chile and Argentina) (Iturraspe, 2016). Patagonian sampling sites were located along a ~428 km north-south transect across three regions: Punta Arenas (PA; 53°17′S, 71°18′W), Karukinka Park (KK; 54°32′S, 68°47′W), and Navarino Island (NI, 54°56′S; 67°53′W) in Chile. PA and NI sites were located on high land whereas KK site was on lowland. MAP (485 mm) and MAT (4.7°C) (Climate normal 1991-2020; CRU TS v.4.05; Table 2.1) show that Patagonian weather is drier than GPB and MG. Among the Chilean Patagonian regions, KK is cooler and

wetter than PA and NI. Patagonian peatlands are dominated by *Sphagnum* mosses (*e.g.*, *Sphagnum magellanicum, S. falcatulum*, and *S. fimbriatum),* perennial herbs (*e.g.*, *Marsippospermum grandiflorum, Tetroncium magellanicum*, and *Rostkovia magellanica*), shrubs (*e.g.*, *Empetrum rubrum* and *Gaultheria pumila)* and lichens. These peatlands are also mostly treeless like their northern counterpart in MG except for scattered dwarf *Nothofagus antarctica* and *N. betuloides* individuals.

2.3.2 Sampling

We sampled water from 73 pools in mid-summer 2019 (July-August in Québec and January-February in Patagonia). Nine pools were sampled in Grande plée Bleue, 38 in the Minganie region, 9 in Punta Arenas, 6 in Karukinka Park, and 11 in Navarino Island. We also conducted inter-annual sampling from 9 pools in Grande plée Bleue in 2019 and 2020 (June to September) to evaluate the temporal patterns of C dynamics in pools.

All water samples were collected from 20 cm below the open-water pool surface at a 2 m distance from the edge of the pools. DOC and DOM samples were collected in 50 mL pre-combusted vials and amber borosilicate vials, respectively, after removing particulate matter through 0.45 µm polyethersulfone (PES) membrane syringe filters. Total phosphorus (TP) and total nitrogen (TN) samples were collected in 50 mL polyethylene (PE) vials, whereas bubble-free pH samples were collected in 15 mL vials. Samples for nitrate (NO_3^-), ammonium (NH_4^+) and phosphate (PO_4^{3-}) analyses were collected in 50 mL PE vials after filtering through 0.2 µm PES membrane syringe filters to remove microorganisms and 6 droplets of 1M H_2SO_4 was added in NO_3^- and NH_4^+ samples to reduce pH below 2. All vials were conditioned with sampling water in the field and all collected samples from Québec and Chilean Patagonia were transported using coolers filled with lots of icepacks to Université de Montréal, Québec, Canada. Collected samples were stored at 4 °C until further laboratory analysis, except for PO_4^{3-} samples which were stored at –20 °C.

The headspace equilibrium technique was used to collect dissolved CO_2 and CH_4 gas samples by taking a 30 mL bubble-free water sample in a 60 mL-syringe and equilibrated with 30 mL ambient air by vigorously shaking for two minutes. Pre-emptied 12 mL exetainer vials (Labco,

UK) were used to transfer the equilibrated 30 mL headspace gas and returned to the laboratory. DO and temperature (T) were measured with a calibrated portable YSI DO200A multimeter (Yellow Spring Instruments, USA). Average pool depth was calculated by dropping the Secchi disk (400g, 20cm diameter) 3-10 times at different locations in the pool based on its size through on-site observation, then averaged. ESRI satellite images (0.46 m resolution) were used in ArcGIS software to measure pool areas. Pool surface elevation was extracted using online GPS visualizer software developed by Adam Schneider (2002) (www.gpsvisualizer.com). Dominant vegetation around the pools was identified through on-site observation. The vegetation cover was described using a modified Braun-Blanquet cover-abundance scale. Ambient temperature and precipitation data (January 1991-December 2020) for all studied sites were compiled from the Climatic Research Unit gridded Time Series (CRU TS) dataset (version 4.05) which was published in July 2021.

2.3.3 Physicochemical analyses

DOC concentration (USEPA-415.1 1974) was measured on filtered water samples using the wet oxidation method with an Aurora 1030 TIC-TOC Analyzer (IO Analytical Instruments, USA) by calculating the difference between total carbon (TC) and inorganic carbon (IC). pH was measured with a calibrated Accumet AB150 pH meter (Fisher Scientific, USA). TP and TN samples were digested using a solution of potassium persulfate and oxidizing reagent (a solution of NaOH and potassium persulfate), respectively. Digested TP and PO_4^{3-} (USEPA-365.1 1993) samples were analyzed on an Astoria 2 segmented flow analyzer (Astoria-Pacific, USA). Digested TN, and acidified NO_3^- (USEPA-352.2 1993) and NH_4^+ (USEPA-350.1 1993) samples analyzed on a Lachat QuikChem 8000 flow injection autoanalyzer (Lachat Instruments, USA).

The collected headspace gas samples were analyzed on a Shimadzu GC-2014 gas chromatograph (Shimadzu Scientific Instruments, USA) equipped with a flame ionization detector (FID) (with attached methanizer) set at 250 ˚C for the detection of CO_2 and CH_4 using a Ni-reduced catalyst column (0.7 m). The concentrations of dissolved CO_2 and CH_4 in pool water were estimated by Henry's law from measured headspace concentrations using headspace equilibrium ratio (1:1 ratio), constant ambient air pCO_2 (411µatm) and pCH_4 (1.9 µatm), and solubility constant for each gas at in situ water temperature. GHG quantity in peatland pool water is presented as CO_2-C and CH_4-C in µg L^{-1}.

2.3.4 Optical analyses

UV-visible absorbance measurements were recorded between 190 and 900 nm using a 10 mm-path quartz cell on a Shimadzu UV-1800 spectrophotometer (Shimadzu Scientific Instruments, USA). Specific UV absorbance ($SUVA_{254}$) was calculated by dividing the UV absorbance at 254 nm (cm^{-1}) by the DOC concentration (mg L^{-1}) and is used as a proxy of DOM aromaticity (Weishaar et al., 2003). The ratio of absorbance at 465 nm to absorbance at 665 nm (E4/E6) was calculated to indicate the well- and less-humified peat condition of the adjacent peatland area of the pool (Turner et al., 2016). DOM fluorescence spectra were scanned using a Varian Cary Eclipse Fluorescence Spectrophotometer (Agilent Technologies, USA) with a 10 mm-path quartz cuvette at room temperature by measuring fluorescence intensity across 220 nm to 450 nm (5-nm increments) excitation wavelengths and 230 nm to 600 nm (2-nm increments) emission wavelengths at 5 nm slit widths.

2.3.5 PARAFAC modeling and DOM components identification and interpretation

Fluorescence spectra were used to conduct PARAFAC analysis on inner-filter effect corrected 156 samples which decompose the excitation and emission matrices by grouping fluorescent compounds with a similar molecular structure into different components (Stedmon et al., 2003) using MATLAB with drEEM toolbox (Murphy et al., 2013). We validated a 3-component PARAFAC model that explained 99.6% of the variation among EEMs data (Table S1 and Figure S1 Supporting Information).

The online repository OpenFluor database was used for the comparison of the PARAFAC components with published studies (Murphy et al., 2014; Table S1 Supporting Information). There were two humic-like components (C1-C2) that have previously been associated to a terrestrial origin. In particular, these two humic-like fluorophores associated with high molecular weight and aromatic compounds have similar spectral features and are most common in freshwater environments (Wauthy et al., 2018; Lambert et al., 2016; Walker et al., 2013; Yamashita et al., 2008). A protein-like component (C3) has been associated to an autochthonous origin from production in the water column, or to recent production in surrounding environments (Stedmon et

al., 2003; Walker et al., 2013; Li et al., 2016). It is typically associated to high biological activity in the environments where it is abundant (Li et al., 2016). In this study, SUVA, E4/E6 ratio and relative abundance of PARAFAC components (%C1-%C2) were used to characterize the DOM quality.

2.3.6 Statistical analyses

Kruskal-Wallis rank tests with Dunn's post hoc tests ($p < 0.05$) were carried out to identify the regional variability of geographical parameters and the spatial and temporal distribution of DOM and GHG. Locally-weighted scatterplot smoothing (LOWESS) with its 95% confidence interval was used to identify and visualize regional patterns of DOM concentrations and compositions, and GHG levels along climate gradients as a function of MAT and MAP. Partial least squares regressions (PLSR) were performed using "pls" r package to identify how morphology, topography, vegetation cover, water chemistry, and DOM composition and concentration influenced the levels of GHG to explore spatial C dynamics among regions and temporal C dynamics within Grande plée Bleue. Non-normalized data of response and explanatory variables were standardized through log transformation. We selected this predictive PLS regression method due to multicollinearity among our variables. We also calculated variable importance in projection (VIP) to identify which variables strongly influenced the GHG concentrations in pools. The R software (R 4.1.0 - R Development Core Team 2021) was used to perform all statistical analyses and graphs.

2.4 Results

2.4.1 Inter-regional patterns in DOM and GHG

DOM concentrations ($p < 0.001$) and humic-like compositions (% C1 & % C2; $p < 0.001$) except protein-like (% C3; $p = 0.18$) showed significant differences among regions, with "PA" having the highest concentrations, while there were no differences within regions in Québec and in Patagonia (Table 2.2). Conversely, although terrestrially derived humic-like components dominated in all regions, peatland pools showed a higher proportion of %C1-%C2 in MG (87.9 ± 3.5%), PA (87.3 ±4.7%) and NI (86.2 ± 3.9%), followed by KK (84.4 ± 6.4%) and GPB (82.4 ± 8.2%) (Table 2.2). The spatial patterns of DOM concentrations and compositions showed larger

variation among regions than within regions and sites from different regions tended to cluster along climate gradients as a function of MAT and MAP (Figure 2.1). MAT systematically explained more variation in DOM concentrations whereas MAP explained more variation in terrestrially derived humic-like (%C1 & %C2) DOM.

All pools were super-saturated in dissolved GHGs relative to the atmosphere, with concentrations ranging from 93.3 to 5388.2 μg L^{-1} and 0.4 to 383.9 μg L^{-1} for CO_2-C (except two pools in MG2, one pool in PA and two pools in NI) and CH_4-C, respectively (Table 2.2). CO_2 was variable within and among regions (between GPB and other regions $p = 0.028$), with GPB having the highest concentrations, while there was no significant difference among MG and Patagonian regions (Table 2.2). CH_4 concentrations showed significant variation between regions in Québec and Patagonia ($p < 0.001$), with higher and more variable concentrations in GPB (Table 2.2). There were only weak relationships between GHG concentrations and MAP and MAT (Figure 2.2).

2.4.2 Influences of geographic properties, environmental conditions and DOM compositions on GHG

The inter-regional patterns observed in DOM (Figure 2.1) and GHG (Figure 2.2) were coherent with inter-regional patterns in geographical and other water chemical and optical variables (Figure 2.3). According to the PLS regression, 35.2% of the variation in CO_2 and CH_4 concentrations, and in CO_2:CH_4 ratio was explained by DOM quality and quantity, water chemistry and geographic properties (Figure 2.3a), with the most variation explained in CO_2 ($R^2 = 0.29$), followed by CH_4 ($R^2 = 0.27$) then CO_2:CH_4 ($R^2 = 0.08$). For instance, pools from GPB as well as few pools from MG tended to cluster toward the top half of Figure 2.3a, along with percent of trees, mosses, and %C3, and concentrations in dissolved CO_2 and CH_4. MG (MG1-MG4) pools were typically found toward the middle of the multivariate space along with higher area and %C2 (Figure 2.3a). Pools in the studied Patagonian regions (PA, KK & NI) were mostly found in the bottom half, along with higher concentrations of DOC and nutrients (TP and TN), %C1, and elevation.

The loading plot (Figure 2.3a) shows that response variables (CO_2 and CH_4) were positively correlated with each other, and they tended to be correlated with similar drivers (Figure 2.3b). The most influential variables (VIP > 1) for both CO_2 and CH_4 concentrations were pools area, humic-

(%C1) and protein-like (%C3) DOM compositions, surrounding vegetation (trees, shrubs, and mosses), and condition of the source peatland area in terms of peat humification (E4/E6) (Figure 2.3). In particular, GHG concentrations increased with decreasing pool area. Humic- (%C1) and protein-like (%C3) DOM composition had a negative and positive effect on GHG concentrations, respectively, but both effects were stronger on CH_4 concentrations (Figure 2.3b). Moreover, decreasing surrounding peat humification (increasing E4/E6 ratio) showed a positive effect on both gases. GHG concentrations were positively correlated with trees and mosses but negatively correlated with shrubs, with CH_4 concentrations having a stronger correlation. On the other hand, water chemical variables *i.e.*, concentrations of DOC and nutrients (TN and TP), had a positive effect on CO_2, but no noticeable influence on CH_4 concentrations (Figure 2.3b). Additionally, CO_2 and CH_4 concentrations exhibited an opposite relationship with pH and elevation.

Table 2.1 Geographical Properties of Peatland Pools (Mean ± SD (Range))

Regions	Sites	Area (m^2)	Depth (cm)	Elevation (m)	Vegetation cover				MAT	MAP
					Trees (%)	Shrubs (%)	Herbs (%)	Mosses (%)	(˚C)	(mm)
Southern	GPB	663±674	129±58	94±0.4	10.3±4.1	32.0±5.8	19.2±11.6	38.3±8.6	3.9	1329
Québec		(72-1897)	(73-219)	(94-95)	(4.2-14.9)	(22.9-43.2)	(5.7-45.7)	(27.0-51.3)		
Minganie	MG1	324±285	47±18	81±0.4	2.9±2.9	20.7±4.4	31.7±6.8	27.4±5.2	1.4	962
		(42-814)	(18-64)	(80-81)	(0-8.9)	(13.4-29.3)	(19.2-40.9)	(20.8-33.3)		
	MG2	4612±7393	43±20	32±0.6	3.0±2.8	25.1±4.8	24.4±5.4	33.7±5.8	1.3	1023
		(355-24542)	(12-77)	(31-33)	(0-7.0)	(18.0-32.0)	(10.7-29.9)	(21.3-44.6)		
	MG3	3316±4076	41±21	30±1	3.3±3.9	19.9±8.9	16.9±6.2	49.1±8.1	1.6	901
		(53-12188)	(14-74)	(29-32)	(0.9-14.3)	(7.1-35.9)	(9.4-26.0)	(35.4-60.3)		
	MG4	1263±1621	54±19	112±0.4	1.8±2.9	16.0±8.2	25.4±6.6	36.7±10.2	-0.2	962
		(67-4143)	(28-81)	(111-113)	(0-10.0)	(9.1-29.6)	(11.6-33.8)	(24.4-61.6)		
Punta Arenas	PA	1120±1752	23±20	266±41	4.5±3.9	17.8±9.8	35.1±6.4	37.0±10.0	5.8	419
		(1-4914)	(5-60)	(224-310)	(1.0-12.2)	(5.8-40.0)	(25.2-44.0)	(22.5-58.6)		
Karukinka	KK	1606±1092	61±48	38±1	2.1±2.5	22.2±6.6	43.9±4.8	24.2±5.5	3.9	537
		(38-2868)	(10-140)	(37-39)	(0.8-7.2)	(16.1-31.9)	(38.9-50.5)	(18.0-32.2)		
Navarino	NI	339±556	26±41	255±109	1.8±2.5	23.5±11.5	25.3±8.9	34.0±13.2	4.3	501
Island		(5-1933)	(4-142)	(33-305)	(0-8.9)	(8.7-41.9)	(11.9-43.7)	(19.4-60.0)		

SD-Standard deviation; MAT-Mean annual temperature; MAP-Mean annual precipitation

Table 2.2 Spatial patterns in DOM and GHG (mean±SD (range)). Different letters denote significant variations among means based on Dunn's post hoc test ($p < 0.05$).

Regions	Sites	DOC (mg L^{-1})	%C1	%C2	%C3	CO_2 -C (µg L^{-1})	CH_4 -C (µg L^{-1})
Southern Québec	GPB	26.4±10.7 (17.0-48.4)^{ac}	49.8±5.0 (37.9-53.9)^{abf}	32.6±5.5 (24.1-40.2)^{abd}	17.5±8.7 (10.0-37.9)^{a}	848.1±383.0 (364.8-1485.4)^{ab}	89.9±129.7 (7.4-383.9)^{a}
Minganie	MG1	20.0±5.5 (13.7-28.9)^{abd}	52.9±2.6 (50.1-56.6)^{bc}	34.2±2.7 (30.9-38.4)^{bcd}	12.8±2.9 (10.0-18.3)^{a}	572.5±222.9 (285.4-967.3)^{bde}	60.6±34.5 (17.2-103.2)^{a}
	MG2	24.0±6.1 (16.4- 35.1)^{ac}	55.0±1.1 (53.3-57.2)^{ce}	36.9±1.1 (35.0-38.8)^{c}	8.0±0.7 (6.9-9.2)^{b}	260.6±98.5 (93.3-381.1)^{c}	11.6±2.8 (7.3-15.2)^{b}
	MG3	13.3±6.3 (6.6-29.2)^{bd}	53.6±1.3 (52.3-56.5)^{ac}	34.2±1.5 (32.1-36.3)^{bcd}	12.1±1.4 (9.4-14.3)^{a}	530.0±443.4 (301.2-1775.5)^{de}	62.7±93.0 (11.4-322.9)^{a}
	MG4	25.7±11.9 (14.8-51.6)^{ac}	49.9±1.9 (45.5-52.5)^{ad}	34.8±3.1 (30.9-42.6)^{bcd}	15.2±3.9 (8.3-22.7)^{a}	463.0±175.4 (237.6-906.4)^{bde}	35.8±29.8 (16.6-116.9)^{ac}
Punta Arenas	PA	43.1±20.9 (19.8-73.0)^{c}	56.4±3.2 (49.1-60.8)^{e}	30.9±3.7 (22.8-36.0)^{de}	12.6±4.7 (7.0-23.0)^{a}	1373.5±1735.0 (199.1-5388.2)^{ae}	32.2±53.6 (2.7-159.3)^{b}
Karukinka	KK	13.6±3.4 (7.9-18.0)^{d}	51.7±3.8 (44.7-55.2)^{cdf}	32.7±4.2 (27.3-40.3)^{de}	15.5±6.4 (9.1-27.8)^{a}	455.8±237.9 (297.9-935.2)^{ce}	4.6±2.8 (0.4-8.0)^{b}
Navarino Island	NI	29.0±12.9 (8.5-54.2)^{ac}	56.6±2.4 (50.4-59.8)^{e}	29.6±1.9 (26.4-32.2)^{e}	13.7±3.9 (8.0-22.7)^{a}	401.3±245.9 (191.6-1021.7)^{ce}	20.7±23.0 (0.8-76.1)^{bc}

SD-Standard deviation

2.4.3 Temporal variation of DOM components and GHG in Grande plée Bleue

Temporal patterns of DOM quantity and quality and GHG concentrations were evaluated throughout the growing season in GPB (Figure 2.4). DOC concentrations ($p = 0.12$; Figure 2.4a) and relative abundance of %C2 ($p = 0.51$) (Figure 2.4b) of DOM components did not show significant temporal variation among months of growing season, whereas %C1 ($p = 0.04$; but June-August were not different; $p = 0.97$) and %C3 ($p = 0.02$) was significantly different across the months (Figure 2.4b). Concentrations of GHG were also more variable among pools than over time within GPB, hence there was temporal pattern in CO_2 concentrations ($p = 0.02$; but June-August were not different; $p = 0.14$; Figure 2.4c) but no temporal variation in CH_4 concentrations ($p = 0.28$; Figure 2.4d).

Water chemistry and DOM composition explained 43.4% of the variation in CO_2, CH_4 and CO_2:CH_4 patterns across the growing season. Figure 2.5a shows that months in the growing summer did not differ from each other, but that for each month the pools covered a wide range of variation. Based on the VIP scores, humic-like DOM composition (%C1), nutrients (TN and TP), DOC concentrations, DO and pH were the most important predictor variables for temporal variation of GHG concentrations (Figure 2.5b). Specifically, GHG concentrations increased with increasing concentrations of DOC and nutrients as well as %C1. In contrast, pH and DO had negative effects on GHG. Moreover, SUVA and % C3 had weak positive effects on GHG and CH_4, respectively.

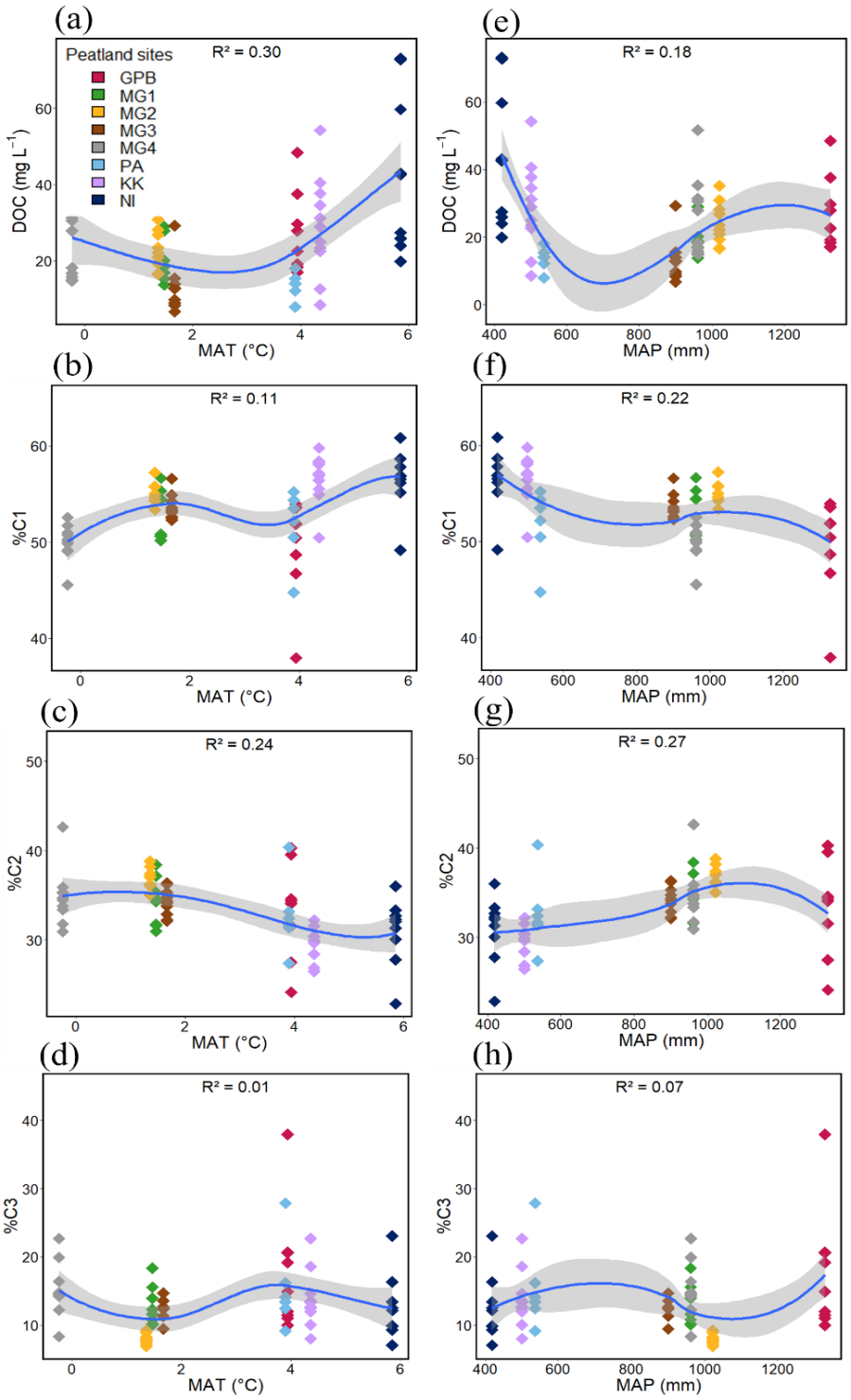

Figure 2.1 DOM concentrations (a, e) and composition (b-d, f-h) patterns in peatland sites across their mean annual temperature (MAT; a-d) and precipitation (MAP; e-h). Dot represents peatland pools (n = 73), and color represents sites (n = 8). Gray regions denote the confidence interval ($p < 0.05$), and the blue lines are the fitted LOWESS smoothing curve.

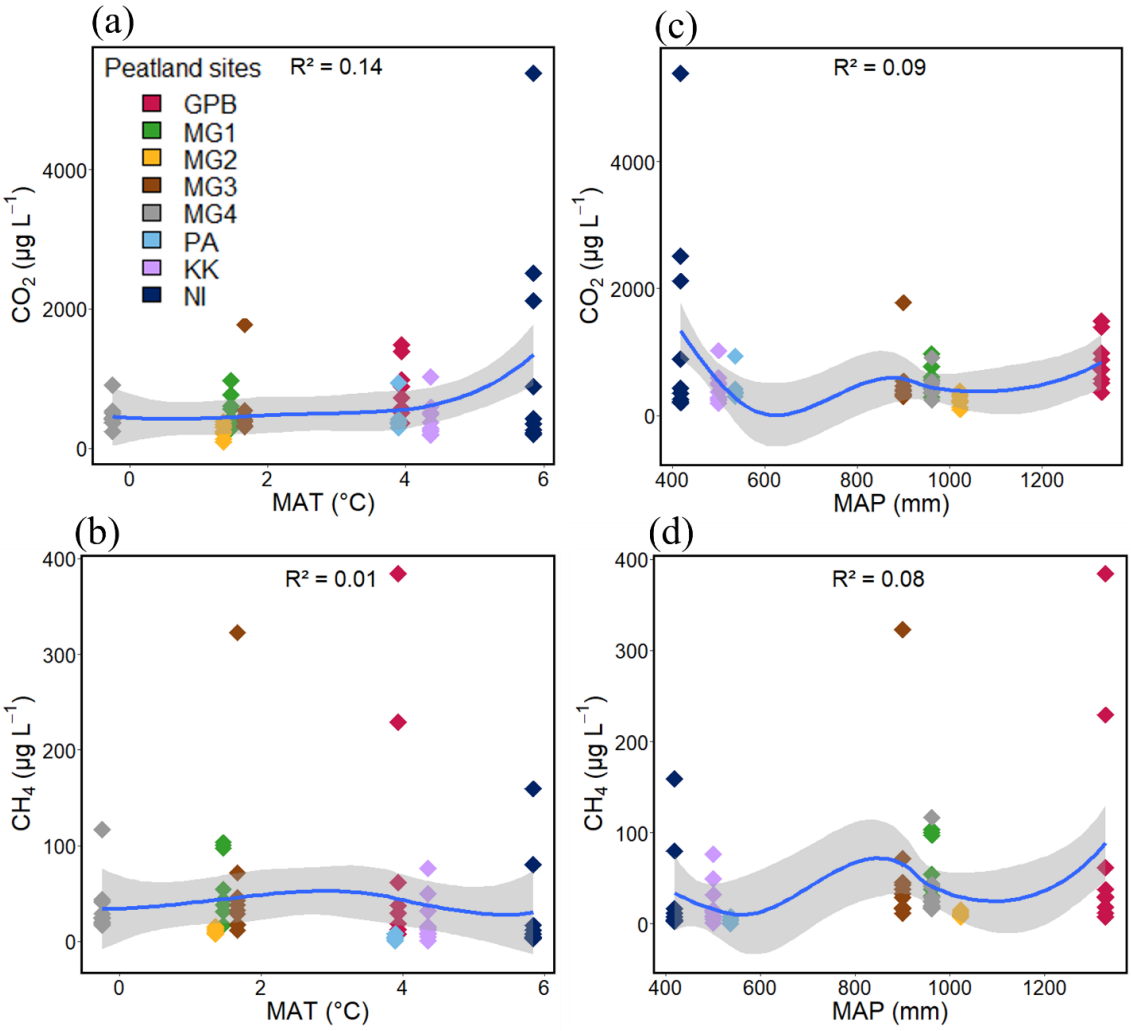

Figure 2.2 Dissolved CO_2 (a,c) and CH_4 (b,d) concentration patterns in peatland sites across their mean annual temperature (MAT; a-b) and precipitation (MAP; c-d). Dot represents peatland pools (n = 73), and color represents sites (n = 8). Gray regions denote the confidence interval ($p < 0.05$), and the blue lines are the fitted LOWESS smoothing curve.

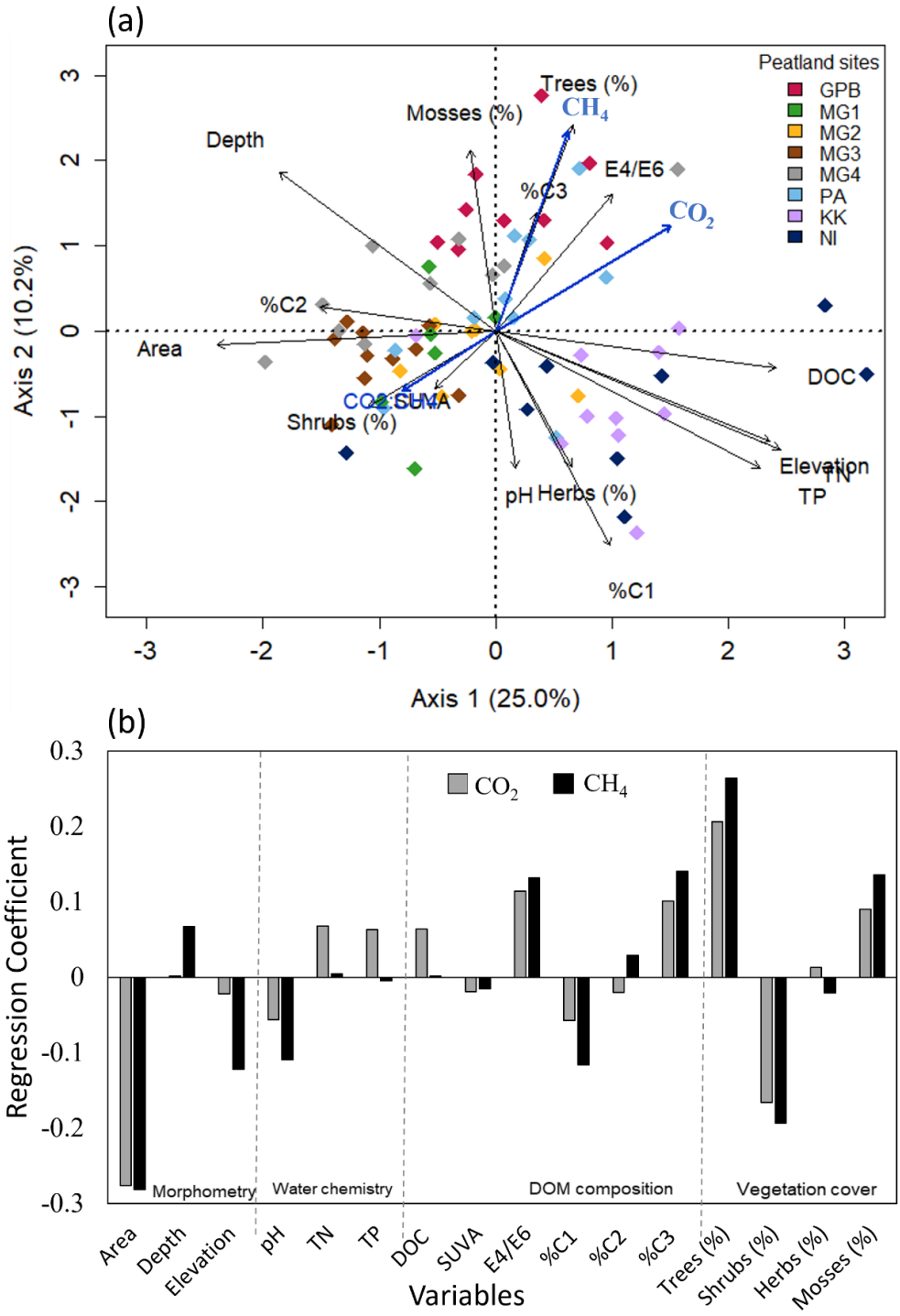

Figure 2.3 In (a), Partial least square regression (PLSR) of CO_2, CH_4, and CO_2:CH_4 gases in relation to the cross-regional geographical and water chemical variables. Variables in black are explanatory variables and those are in blue, response. The dot colors represent the peatland sites. In (b), Regression coefficient from PLSR for the explanatory variables for each gas.

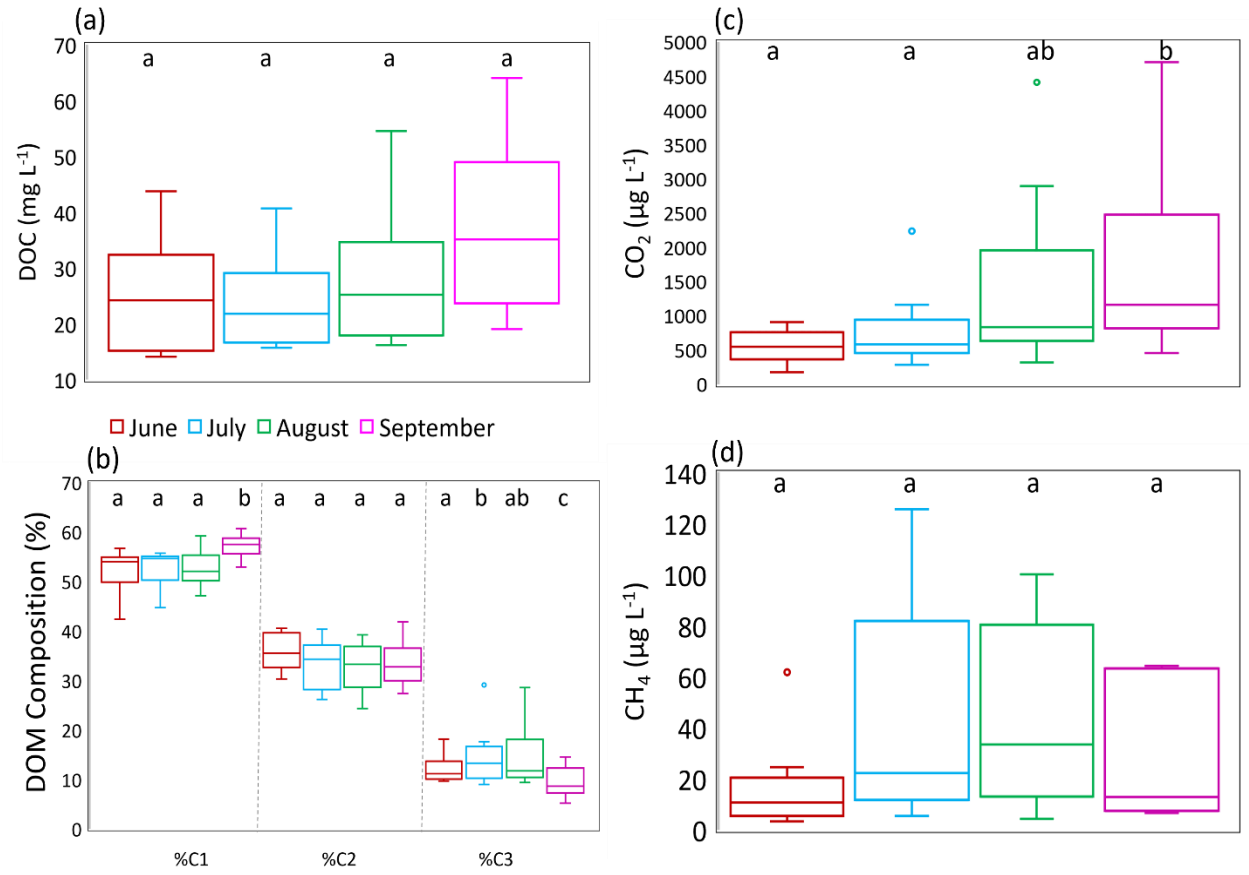

Figure 2.4 Seasonal patterns in DOM and GHG in Grande plée Bleue. In (a), boxplot of DOC concentration, in (b), relative abundance of DOM composition, and in (c-d), CO_2 and CH_4 concentrations. Boxes show the median and 25-75th percentiles, and whiskers show the 10-90th percentiles. Box color represents the months. Different letters denote significant variations among means based on Dunn's post hoc test ($p < 0.05$).

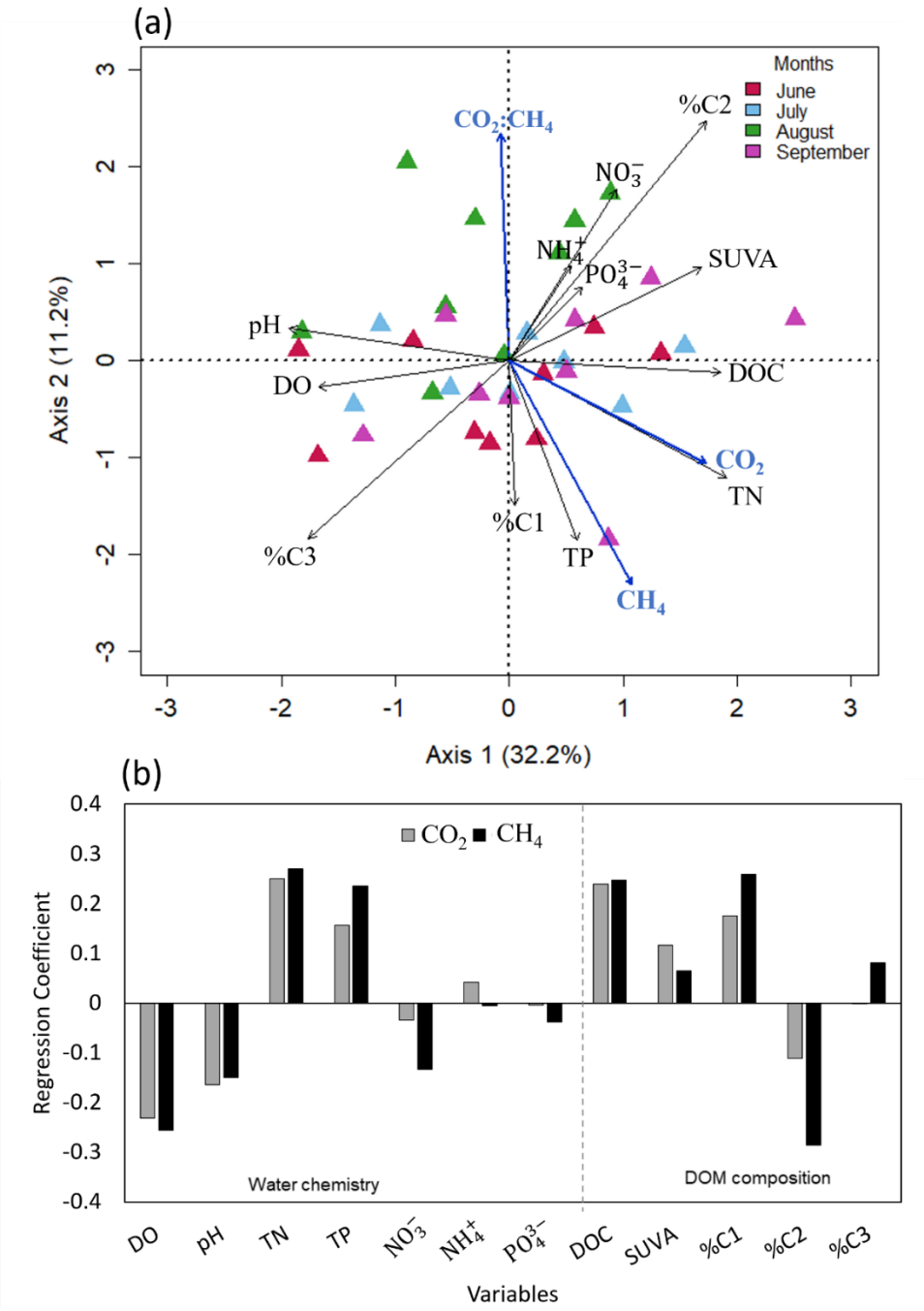

Figure 2.5 In (a), Partial least square regression (PLSR) of dissolved CO_2 and CH_4 concentrations, and CO_2:CH_4 in relation to the temporal water chemical variables and DOM compositions in Grande plée Bleue. Variables in black are explanatory variables and those are in blue, response. Dot represents pools (n = 9) and dot color represents months (June to September). In (b), regression coefficient from PLSR for the explanatory variables for each gas. Gray column represents CO_2, whereas black represents CH_4.

2.5 Discussion

In this study, we found spatial patterns in DOM and GHG in peatland pools that were consistent among regions. These patterns were associated with inter-regional patterns in climate and pool morphometry, vegetation cover, and the predominance of protein-like DOM in the water. The spatial variability among pools in GPB was higher than the temporal variability in that region, indicating local-scale controls on temporal peatland pool biogeochemistry. DOC concentrations were positively correlated with MAT (Figure 1a) but inversely correlated with both area and depth of pools (Figure 3a). This could be explained by higher production and leaching of DOC in and from the peat at higher temperatures (Freeman et al., 2001). These differential inputs and processing rates appeared to impact DOM composition, as %C1 tended to increase as a function of MAT and decrease as a function of MAP, a pattern that was inverse compared to %C2 (Figure 1). The similar pattern between DOC and %C1 suggests that most of the DOC is composed of C1 and that C1 predominately originates from the peat. The weak relationship between percent of protein-like C3 and climate variables suggests that it may follow a more local behavior tied to rapid in-pool production and uptake, as has been shown in other types of aquatic ecosystems (Lapierre & del Giorgio, 2014). The range of DOC concentrations (Table 2.2) in this study are comparable to those from peatland pools in the UK and Canada (Turner et al., 2016; Pelletier et al., 2014; Billett & Moore, 2008; Hamilton et al., 1994). DOC concentrations in this study are also within the range of those found in small peatland lakes in boreal western Canada (Kuhn et al., 2021). The effects of climate and landscape position on inter-regional patterns in DOM could thus be mediated by their influences on the vegetation composition and peat characteristics of peatlands.

At the regional scale, DOM quality may primarily depend on the type of surrounding vegetation, while its concentration depends on the morphometry of pools. The higher absolute concentrations and relative abundance of humic-like DOM (C1 and C2) that we typically observed across regions (Figure 1; Table 2; Table S2 in Supporting Information) indicate high terrestrial inputs from the surrounding peat at all sites. A strong positive relationship was found between humic-like DOM compositions and SUVA (Figure 2.3a), suggestive of high molecular weight and aromaticity (Helm et al., 2008). At GPB, Arsenault et al. (2018) previously measured higher SUVA in peatland pools surrounded by trees and shrubs plants (trees>shrubs>herbs>mosses).

Here, we found relatively homogeneous values among the regions ($p = 0.88$; Table S2 in Supporting Information S1) that could be explained by a similar dominance of mosses across regions (Table 2.1). The protein-like DOM composition (%C3) had a positive relationship with relative trees and mosses cover and peat humification index (E4/E6 ratio), suggesting that this component may also originate from freshly produced terrestrially-derived DOM (Yamashita et al., 2013; Lapierre et al., 2013; Amaral et al., 2021).

A combination of geographic (climate, morphometry, vegetation cover) properties, water column properties and DOM composition influenced the cross-regional patterns in dissolved GHG in peatland pools. Pools were typically supersaturated in dissolved CO_2 and CH_4 (Table 2.2), and GHG concentrations were mostly within the range of those previously reported for pools and small lakes in peatlands (Turner et al., 2016; Pelletier et al., 2014; Repo et al., 2007, Hamilton et al., 1994). The regional variability of CO_2 and CH_4 concentrations (Figure 2.2) could be explained by direct and indirect climate effects. we found no strong relationship between long-term averages in MAT and MAP (Figure 2.2) which was surprising since warmer temperatures can enhance GHG production (especially CH_4) in the bottom anoxic sediments by stimulating the activities of methanogens (Kuhn et al., 2021). It might be because of short-term variations in weather, or it is mediated by more proximal factors directly associated to gas production and loading mechanisms in or around pools. An alternative source of GHG in peatland pools is the direct input of CO_2 and CH_4 from peat rather than produced in the anoxic sediments of the pool (Billett et al., 2004). The strong positive relationship between peat characteristics (E4/E6 ratio) and GHG levels suggests that peat-produced GHG could have been imported into peatland pools along with peat-derived DOC. Low humification of surrounding peat and small pool size in GPB compared to other regions suggest that there may be higher hydraulic connectivity between peat and pools in this region (Billett et al., 2012), influencing peat-produced GHG transport to the pools. Our findings of increasing CO_2 and CH_4 concentrations with higher tree abundance suggest that root exudate and litter deposition may stimulate the inputs of freshly produced and bio-labile DOM from peat to water (Hoyos-Santillan et al., 2016), increasing biological activity in pools. Inter-regional patterns in climate and in peat characteristics may thus drive spatial patterns in the inputs of DOM and GHG from peat to water, as well as in situ production of DOM and GHG within pools. However, further study is required to identify how peat properties (i.e., peat structure and biogeochemical

characteristics) and hydrological connectivity influence the pool C biogeochemistry by transporting DOM and peat-produced GHG using molecular analysis.

Pool area was the most important morphological driver of GHG patterns, with a negative effect on the levels of both CO_2 and CH_4. Reasons behind the high GHG concentrations in small pools compared to larger pools could include high terrigenous C loading relative to water volume, high perimeter to area ratio, and low water depth (Holgerson 2015; Holgerson and Raymond, 2016; Wik et al., 2016). These factors would favor higher direct inputs of peat-derived GHG, and stimulate in situ production of GHG through increased DOM inputs. At the inter-regional scale, depth did not show any relationship with GHG concentrations, a pattern opposed to the findings of Arsenault et al. (2018) within the GPB peatland pools. Our results thus suggest that the high inter-regional variation in climate, vegetation and pool area in the sampled pools overwhelms the local variation in depth in driving peatland pools C biogeochemistry over broad spatial extents.

We found that GHG most strongly correlated with autochthonous or freshly produced allochthonous DOM across the studied sites. Our findings of decreasing CO_2 and CH_4 concentrations in peatland pools with higher humic-like DOM composition contrast previous studies in lake, stream, river, and estuary (D'Amario & Xenopoulos, 2015; Zhou et al., 2018; Amaral et al., 2021), where high inputs of terrestrial DOM may correlate with hydrological inputs of terrestrially produced GHG, and where terrestrial DOM itself may serve as an important substrate for mineralization to CO_2 within the aquatic environment. We suggest that this discrepancy may have occurred because of different hydrological settings, morphometry, loading of terrestrial DOM and nutrient limitation in peatland pools compared to these previously studied systems. A recent study conducted on peatland lakes found an inverse relationship between DOC and CO_2 concentrations (Kuhn et al., 2021), which may be explained by the fact that increasing terrestrial-derived DOM may not significantly influence microbial respiration compared to its stimulating effect on aquatic primary production. This reasoning is coherent with the fact that protein-like DOM composition (%C3) appeared to positively influence the cross-regional spatial distribution of dissolved CO_2 and CH_4 concentrations in peatland pools. This protein-like DOM may originate from high phototrophic and heterotrophic activity in the water or at the water-peat interface, or be loaded from the surrounding peat under conditions of high production or

mobilization of DOM from peat to water. A previous study has found that presumed high input of freshly produced DOM (in the water or on land) in wetlands may sustain high proportions of protein-like DOM (Lapierre & del Giorgio, 2014), although this DOM may differ from Sphagnum-produced DOM. Aquatic microbial communities then preferentially consume and respire this protein-like DOM due to its high accessibility and nutrient quality (Kritzberg et al., 2004; Guillemette et al., 2016), potentially leading to high levels of CO_2 production. On the other hand, methanogenesis in anoxic C-rich sediment is the main pathway of biological CH_4 production in aquatic environments (Michaud et al., 2017). Intrinsic algal-derived DOM can also be preferentially bio-labile for the microbial community in an anoxic environment (Zhou et al., 2018) and likely enhance methanogenesis (Bogard et al., 2014). Our findings thus suggest that a higher abundance of protein-like, freshly-produced DOM in peatland pools lead to higher biological activity, hence to higher GHG production and concentrations.

At the temporal scale, pool morphometry appears as the main driver of the observed seasonal patterns of DOM in peatland pools. DOC and %C1 tended to increase with progressing growing seasons (Figure 2.4a-b), but only the month of September was significantly different from other months due to large pool-to-pool variation. In GPB, terrestrial DOM and nutrients are known to be transported from surrounding peat to pools throughout the summer due to higher water table amplitude and rapid response rates to precipitation events in peat compared to pool water level (Arsenault et al., 2019). On the other hand, protein-like DOM (%C3) showed significant temporal changes with the highest values during mid-summer (July-August). Primary production (algae and cyanobacteria) may be increased in the limnetic bottom peat of pools due to the availability of light, oxygen, and nutrients (Hamilton et al, 1994), resulting in higher autochthonous DOM, but this has not been measured. Moreover, runoff from peat to pool (as autochthonous C3 was associated with freshly produced terrestrial DOM) and evaporation may be other phenomena for higher %C3 during mid-summer. CO_2 tended to increase over months and reached a maximum in September, similar to DOC and %C1, but CH_4 followed a pattern that more closely matched temporal variation in protein-like %C3 DOM. Unlike C3, however, this pattern was not significant, because variation among pools at any moment is higher than variation within a single pool over time. At the intra-regional scale, higher inputs of DOM and nutrients from peat to water are a stronger driver of GHG patterns than the proportion of protein-like DOM, suggesting different

controls on GHG dynamics across spatial and temporal scales. It appears that increasing water temperature, nutrients, and high loading of DOM from surrounding peat during the growing season may create an environment for elevated biological and photochemical production of GHG in the pools, as well as be a proxy of the input of GHG from the surrounding peat. Moreover, high peat loading DOM and degradation processes in water create a favorable anoxic environment for methanogens by driving pH and DO levels down and leading to high in situ CH_4 production in pools (Figure 2.5b). Among pools, however, humic-like DOM composition explained a larger proportion of CH_4 temporal pattern than the protein-like DOM. Recent studies found that high content of terrestrial derived DOM contributes to methanogenesis along with algal derived autochthonous DOM (Araujo et al., 2018). Moreover, peat-produced GHG may be imported via runoff (Wehhenmeyer et al., 2015; Paytan et al., 2015) throughout the growing season explaining in part the elevated CO_2 and CH_4 levels that were observed in this study, but evidence remains rare for hydrological gas input from peat to pools.

2.6 Conclusion

Peatlands are important players in the global C budget (Yu et al., 2011; Waddington & Roulet, 2000; Frolking et al., 2001), and the C dynamics in pools can to some level counter-balance the net role of peatlands as sinks (Pelletier et al., 2015). While there is a rich literature on the aquatic C cycling in lakes and rivers, this knowledge cannot be readily transposed to peatland pools because they occupy a very different biogeochemical space compared to other lentic ecosystems (Arsenault et al., 2022). We found that local scale drivers such as pool morphometry predominantly control intra-regional, temporal patterns in DOM and GHG, while broad scale climate and vegetation cover drive inter-regional patterns in DOM, GHG and the links among them. The predominant role of climate, whether it is direct or indirect, on inter-regional patterns suggests that more studies are needed in regions with contrasting temperature, precipitation and vegetation cover. This is important as broad scale patterns in DOM and GHG vary depending on the variable considered and are non-linear as a function of climate, limiting prediction of the changing role of peatland pools in the global C cycle under rapid environmental changes.

2.7 Acknowledgment

We wish to express our deepest sincere thankfulness to Dominic Bélanger for laboratory support. We express thanks to the Société de conservation et de mise en valeur de la Grande plée Bleue for giving permission us to conduct our research in this peatland. We also thank members of the Talbot and Lapierre lab for sample collection, laboratory analysis, and statistical and writing help. This research was funded through NSERC Discovery Grant to Jean-François Lapierre and Julie Talbot, FRQNT Relève Professorale to Jean-François Lapierre, Groupe de Recherche Interuniversitaire en Limnologie (GRIL) and FRQNT Regroupements Stratégiques MSc fellowship to Mahmud Hassan.

2.8 Data availability statement

Data used in this study are available on borealisdata.ca (https://doi.org/10.5683/SP3/CJH4YV).

2.9 Supporting information

This supporting information contains figure of and tables of methodology and results. A 3-component PARAFAC model were performed and validated to identify the dissolved organic matter (DOM) component in peatland pool (Figure S1). Online OpenFlour database (https://openfluor.lablicate.com) of DOM components were used to identify their characteristics and sources as well as number of matchings with previous studied components (Table S1). In Figure S1 and Table S1, C1 and C2 represent terrestrially derived humic-like DOM, and C3 represents protein-like component associated with freshly produced DOM. Table S2 shows the inter-regional patterns in chemical and optical properties of peatlands pools across five geographically diverse regions.

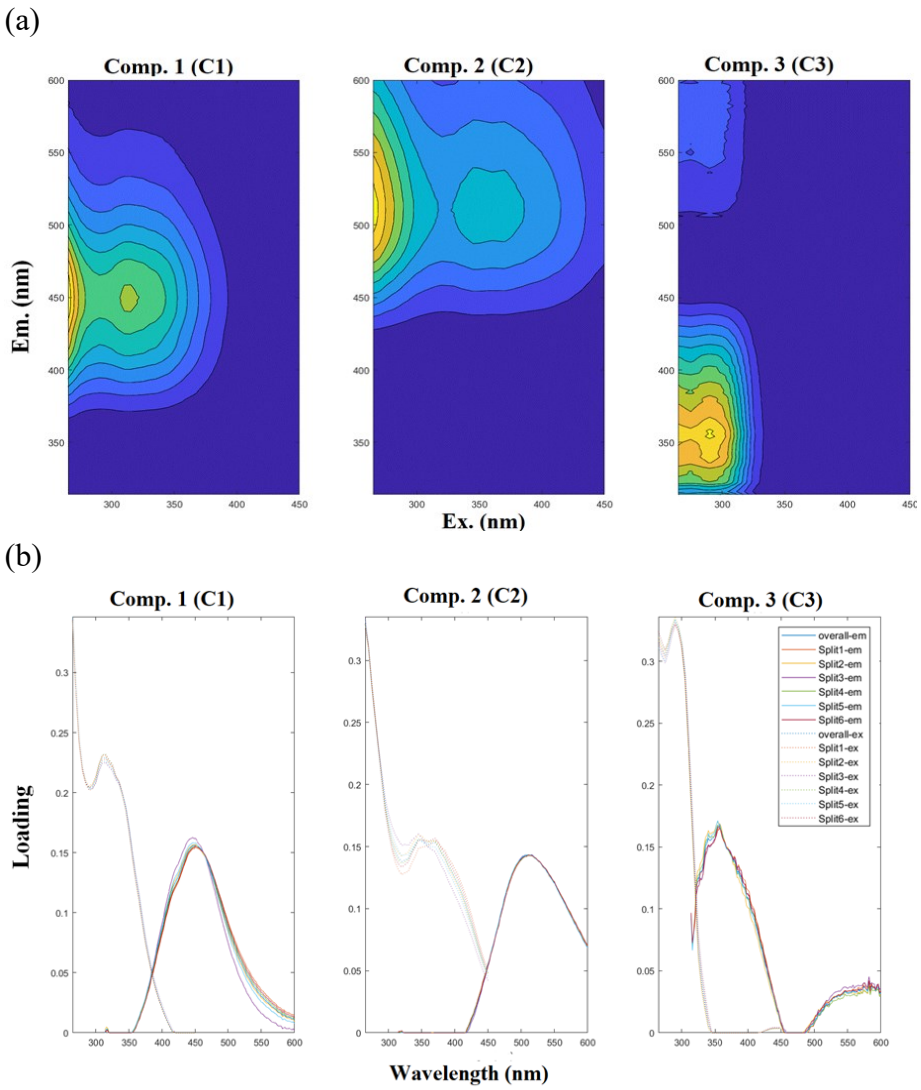

Figure S1. Excitation and emission matrices of PARAFAC components. (a) Contour plots for 3-component PARAFAC model; (b) split-half validation plots for PARAFAC components.

Table S 1. Identification of validated PARAFAC components using spectral characteristics and number of matches with OpenFluor database (minimum similarity of 0.95).

Component	Maximum excitation (nm)	Maximum emission (nm)	Number of *OpenFluor matches*	sources
C1	<265 (310)	450	65	Humic
C2	<265	510	64	Humic
C3	290	354	34	Protein

Table S 2. Spatial patterns of water chemical and optical parameters (mean±SD (range)). Different letters denote significant variations among means based on Dunn's post hoc test ($p < 0.05$).

Regions	Sites	TP (μg L^{-1})	TN (mg L^{-1})	SUVA (L mgC^{-1} m^{-1})	E4/E6 ratio	C1 (RU)	C2 (RU)	C3 (RU)
Southern Québec	GPB	15.78±3.61 (10.70-21.27) ^{ad}	0.68±0.28 (0.38-1.22) ^{a}	3.51±0.91 (1.67-4.53)^{a}	4.70±1.38 (3.22-7.71)^{a}	5.13±2.36 (2.06-8.86)^{abc}	3.51±2.05 (1.09-7.33) ^{ab}	1.67±0.81 (0.76-2.84) ^{a}
Minganie	MG1	17.10±10.41 (9.37-34.64) ^{ab}	0.78±0.29 (0.37-1.22) ^{ad}	3.42±0.45 (2.64-4.01)^{a}	1.63±0.19 (1.4-2.0)^{b}	4.69±1.84 (2.87-8.52)^{bc}	3.01±1.03 (1.75-4.77) ^{bd}	1.07±0.28 (0.87-1.74) ^{ac}
	MG2	10.79±3.02 (6.64-17.71) ^{b}	0.51±0.10 (0.35-0.73) ^{a}	4.45±0.17 (4.21-4.70)^{b}	2.11±0.16 (1.90-2.37)^{bc}	5.88±1.61 (3.93-8.87)^{b}	3.91±0.92 (2.67-5.43) ^{b}	0.84±0.20 (0.59-1.20) ^{bce}
	MG3	17.12±14.51 (8.74-56.66) ^{bc}	0.68±0.50 (0.30-1.86) ^{a}	3.96±0.78 (3.37-6.04)^{ab}	3.34±2.02 (1.27-6.0)^{cd}	3.17±1.74 (1.53-7.41)^{cd}	1.99±0.96 (0.93-4.21) ^{acd}	0.70±0.34 (0.41-1.48) ^{b}
	MG4	14.29±2.31 (10.52-18.33) ^{ac}	0.59±0.29 (0.35-1.37) ^{a}	1.83±0.78 (0.86-3.37)^{c}	4.0±0.77 (2.5-5.0)^{ad}	1.90±0.47 (1.47-3.01) ^{d}	1.33±0.39 (0.92-2.03) ^{c}	0.56±0.12 (0.39-0.79) ^{b}
Punta Arenas	PA	91.63±126.71 (15.19-408.65) ^{d}	1.30±0.66 (0.63-2.60) ^{b}	3.50±0.39 (2.98-4.05)^{a}	2.80±0.94 (1.93-4.83)^{cde}	12.77±9.59 (3.69-31.38)^{be}	6.62±4.22 (2.19-11.78) ^{be}	2.64±2.34 (0.81-8.43) ^{a}
Karukinka	KK	12.23±8.03 (6.93-28.31) ^{bce}	0.51±0.23 (0.38-0.98) ^{ac}	3.45±0.34 (2.75-3.67)^{a}	1.93±1.34 (1.27-4.66)^{bf}	2.56±0.68 (1.42-3.42) ^{cdf}	1.66±0.63 (0.80-2.74) ^{cf}	0.76±0.36 (0.34-1.44) ^{bcd}
Navarino Island	NI	54.80±88.52 (11.71-316.54) ^{d}	1.32±0.87 (0.56-3.60) ^{bd}	3.23±0.44 (2.11-3.71)^{ac}	3.67±1.19 (2.0-5.71)^{ade}	6.69±3.68 (1.30-14.18) ^{be}	3.49±1.92 (0.69-7.64) ^{be}	1.49±0.80 (0.54-3.45) ^{ae}

Note: SD- standard deviation

Chapter 3: General Conclusions

3.1 Review of the objectives of this study

The main objective of this project was to understand and quantify the intra- and inter-regional patterns and drivers of GHG (CO_2 and CH_4) and DOM concentrations and composition in peatland pools as well as their links in changing geographical conditions (*i.e.*, climate, vegetation cover and pools morphometry) across five areas of northern (Québec, Canada) and southern (Chilean Patagonia) hemisphere. Few studies have been conducted in pools and small lakes in peatland focusing on the spatial distribution of GHG concentrations (Turner et al., 2016) and emissions (Kuhn et al., 2021) at the inter-regional scale, but the inter-regional patterns of DOM and their role in GHG production in peatland pools remain entirely unexplored. We analyzed a range of optical and chemical variables controlling GHG and DOM concentrations and composition in peatland pools across studied sites, combined with inter-annual sampling in Grande plée Bleue in 2019 and 2020 (June to September). We performed and validated a 3-component PARAFAC model to identify the DOM component in peatland pool. These results were then combined with geographic properties data to identify the patterns of DOM and GHG in studied sites and regions. We used statistical analyses to identify how DOM composition and concentration along with other water chemical properties as well as geographic properties influence CO_2 and CH_4 concentrations in peatland pools.

3.1.1 Internal and external drivers of spatial and temporal patterns of DOM and dissolved GHG

The first goal of this project was to observe and understand which external and internal drivers control the intra- and inter-regional distribution of DOM and GHG in peatland pools. We hypothesized that spatial heterogeneity of DOM and GHG concentrations depend on the variation of climate, morphology, vegetation cover and water chemistry, whereas DOM quality depends on the type of vegetation cover. Overall, our research shows that inter-regional variability of DOM quality and quantity and GHG concentrations is high compared to intra-regional variability which is coherent with the heterogeneity of geographical properties. DOM concentrations and terrestrial humic-like (%C1) composition tend to increase with elevated MAT and decrease as a function of MAP. We found a weak relationship between protein-like DOM compositions, GHG

concentrations, and climate variables which suggests that they are more related to and driven by short-term variations in weather. The pool area significantly inversely influences the concentrations of both DOM and GHG (*i.e.*, CO_2 and CH_4). Moreover, the abundance of trees and mosses shows a significant positive relationship with protein-like DOM compositions and GHG concentrations which suggests that root exudate and litter deposition may stimulate the inputs of freshly produced bio-labile DOM from peat to water, increasing GHG production through stimulating biological activity in pools. Although a direct correlation between humic-like DOM composition and vegetation might have been expected, our results suggest that this was not the case for the complex mixtures analyzed in this study.

Another goal of this project was to identify temporal patterns and drivers of DOM and GHG in peatland pools and hypothesized that their concentrations may be higher in wet periods than dry periods due to local variation in weather, hydrological connectivity, and water chemistry. But we did not find significant temporal patterns in any aspect of C cycling (except protein-like DOM composition), and that suggests that the main source of variation is from pool to pool. Figure 2.5a shows the months in the growing season did not really differ from each other, but that for each month the sites covered a wide range of variation, and it was in pools with typically high concentrations of DOM and nutrients, among all months, that GHG were the highest. In this study, we showed temporal variation in only one studied site which should not be assumed to be representative of other regions. However, further large-scale temporal analysis is required across geographically diverse sites to explore proper temporal patterns and understand the controls on the variability of the carbon cycle in peatland pools.

3.1.2 The role of DOM on GHG in peatland pools at the spatial and temporal scales

The last goal of this study was to evaluate the role of DOM, an important intermediate of carbon dynamics, on GHG production in peatland pools. We hypothesized that DOM concentration and composition both have an effect on GHG concentrations, but this effect is different depending on the scale considered. We found terrestrially derived humic-like components dominated in all regions (average ~85.6%; Table S2) and expected positive relation with GHG concentrations according to our hypothesis and previous studies in different aquatic environments (Amaral et al.,

2021; Zhou et al., 2018; D'Amario & Xenopoulos, 2015). But surprisingly, our results indicated that dissolved GHG increased with autochthonous protein-like DOM and decreased with allochthonous humic-like DOM at an inter-regional scale (Figure 2.3b). We suggest that high drainage ratio and hydrological connectivity with peat lead to high loading of terrestrial DOM in peatland pools which may not influence the microbial respiration due to lack of nutrients and serves as an important substrate for mineralization to CO_2. High loading of terrestrial DOM may correlate with hydrological inputs of peat-produced GHG in peatland pools, although this was not measured directly in this study. On the other hand, autochthonous protein-like material associated with freshly produced or imported DOM may be preferentially consumed and respired by microbial communities in both oxic and anoxic environments due to their high nutrient quality and accessibility, which may lead to higher production and concentrations of CO_2 and CH_4 in peatland pools. At the temporal scale, we found the opposite trend of the relationship between terrestrial-derived humic-like DOM and GHG as what we expected for the cross-regional scale (Figure 2.5b).

3.2 Study prospects

Recently, the study of C dynamics in peatland pools has been getting attention (e.g., Kuhn et al., 2021; Arsenault et al., 2018; Turner et al., 2016; Wik et al., 2016; Pelletier et al., 2014; McEnroe et al., 2009; Repo et al., 2007; Waddington & Roulet, 2000; Hamilton et al., 1994) along with peatlands' vegetated surfaces because of their high C emission rate (especially CH_4) to the atmosphere compared to other types of small waterbodies (Wik et al., 2016) and their important role as a net C emitter in the contemporary C budget in the net C sink peatland ecosystems (Pelletier et al. 2015). For example, peatland pools cover 8-12% of the surface area in Hudson Bay Lowland but emit 30% of CH_4 (Hamilton et al., 1994). Moreover, a peatland can be a net C source if peatland pools occupy 37% of the total surface area (Pelletier et al., 2014). But there is a glaring lack of empirical data about the intermediary form of C i.e., DOM, and its role in the production of GHG in peatland pools. To our knowledge, this study has provided the first detailed insight into inter-regional variation in DOM quality and quantity, and their links with GHG (CO_2 and CH_4) concentrations in ombrotrophic bog pools. The studied ombrotrophic peatland sites are geographically (climate, topography, morphology, and vegetation cover) diverse. Unsurprisingly, bogs are dominated by sphagnum mosses and characterized by relatively shallow (in comparison to larger water bodies) dystrophic peatlands pools with acidic water due to high levels of dissolved

humus, and low nutrient contents (Arsenault et al., 2018; Turner et al., 2016; Beadle et al., 2015). However, there are also some significant specific differences in the water chemistry among sites and regions that have implications for biogeochemical processes and C cycling. Our results suggest that broad scale patterns in geographic properties (climate, vegetation cover and pool morphometry) predominantly control the cross-regional patterns in DOM and GHG and their links, while local scale drivers such as pool morphometry predominantly influence the temporal variations in DOM and GHG. Protein-like DOM appears as an indicator of biological activity and within pool GHG production across regions, while humic-like DOM appears as an indicator of DOM and GHG loadings from peat to pools at the intra-regional scale.

This study improves the prediction and understanding of the role of peatland pools in the global C cycle under rapid environmental changes and suggests that peatland pools should be considered separately from other types of small waterbodies during the future study of C dynamics (see Arsenault et al. 2022) due to higher loading of terrestrial C, organic-rich peat bottom, and hydrological connectivity between peat and pool. However, further global-scale assessment of C dynamics in peatland pools is required to understand and identify the actual role in the global peatland C cycle across all climatic regions by considering their regional climate, landscape position, catchment properties (vegetation cover, peat biogeochemistry and hydrological connectivity) and morphological characteristics as well as in situ pool chemistry. Large-scale temporal analysis is also required across geographically diverse regions to explore proper temporal patterns and understand the controls on the variability of the C cycle in peatland pools. To properly understand and evaluate the relation between DOM and GHG production, our research raises the following further research goals.

- Identify the alteration of DOM compositions in peat and pools due to photo- and bio-degradation and subsequent GHG production as a consequence in different geographically diverse regions.
- Identify how peat properties (i.e., peat structure and biogeochemical characteristics) and hydrological connectivity influence the DOM quality in the peat-pool interface using molecular analysis.

- Identify the distribution of microbial communities and their promoting drivers in peat and pools, and their roles in GHG production through biodegradation in oxic and anoxic environments.

Moreover, further studies require evaluating the global abundance and total surface area of peatland pools to get their true role in the global peatland ecosystems as well as the global C budget.

References

Algesten, G., Sobek S., Bergstrom, A-K., Anders Jonsson A., Lars J. Tranvik, L.J., & Jansson, M. (2005). Contribution of Sediment Respiration to Summer CO2 Emission from Low Productive Boreal and Subarctic Lakes. *Microbial Ecology*, 50, 529-535. https://doi.org/10.1007/s00248-005-5007-x

Amaral, V., Ortega, T., Romera-Castillo, C., & Forja, J. (2021). Linkages between greenhouse gases (CO_2, CH_4, and N_2O) and dissolved organic matter composition in a shallow estuary. *Science of the Total Environment*, 788, 147863. https://doi.org/10.1016/j.scitotenv.2021.147863

Araujo, J., Pratihary, A., Naik, R., Naik, H. & Naqvi, S.W.A. (2018). Benthic fluxes of methane along the salinity gradient of a tropical monsoonal estuary: implications for CH_4 supersaturation and emission. *Marine Chemistry*, 202, 73-85. https://doi.org/10.1016/j.marchem.2018.03.008

Arsenault, J., Talbot, J., Brown, L.E., Holden, J., Martinez-Cruz, K., Sepulveda-Jauregui, A., Swindles, G.T., Wauthy, M., & Lapierre, J.-F. (2022). Biogeochemical distinctiveness of peatland ponds, thermokarst waterbodies and lakes. *Geophysical Research Letters*, 49(11), e2021GL097492. https://doi.org/10.1029/2021GL097492

Arsenault, J., Talbot, J., Moore, T.R., Beauvais, M-P., Franssen, J., & Roulet, N.T. (2019). The spatial heterogeneity of vegetation, hydrology and water chemistry in a peatland with open water pools. *Ecosystems*, 22, 1352-1367. https://doi.org/10.1007/s10021-019-00342-4

Arsenault., J., Talbot, J., & Moore, T.R. (2018). Environmental controls of C, N and P biogeochemistry in peatland pools. *Science of the Total Environment*, 631-632, 714-722. https://doi.org/10.1016/j.scitotenv.2018.03.064

Aufdenkampe, A.K., Mayorga, E., Raymond, P.A., Melack, J.M., Doney, S.C., Alin, S.R., Aalto, R.E., & Yoo, K. (2011). Riverine coupling of biogeochemical cycles between land, oceans, and atmosphere. *Frontiers in Ecology and the Environment*, 9(1), 53-60. https://doi.org/10.1890/100014

Bange, H.W., & Uher, G. (2005). Photochemical production of methane in natural waters: implications for its present and past oceanic source. *Chemosphere*, 58(2), 177-183. https://doi.org/10.1016/j.chemosphere.2004.06.022

Bengtsson, F., Rydin, H., Baltzer J.L., Bragazza, L., Bu, Z-J., Caporn, S.J.M., et al. (2020). Environmental drivers of *Sphagnum* growth in peatlands across the Holarctic region. *Journal of Ecology*, 109(1), 417-431. https://doi.org/10.1111/1365-2745.13499

Biggs, J., von Fumetti, S., & Kelly-Quinn, M. (2017). The importance of small waterbodies for biodiversity and ecosystem services: implications for policy makers. *Hydrobiologia*, 793, 3-39.

Billett, M.F. & Moore, T.R. (2008). Supersaturation and evasion of CO_2 and CH_4 in surface waters at Mer Bleue peatland, Canada. *Hydrological Processes*, 22(12), 2044-2054. https://doi.org/10.1002/hyp.6805

Billett, M.F., Deacon, C.M., Palmer, S.M., Dawson, J.J.C., & Hope, D. (2006). Connecting organic carbon in stream water and soils in a peatland catchment. *Journal of Geophysical Research: Biogeosciences*, 111(G2), G02010. https://doi.org/10.1029/2005JG000065

Billett, M.F., Dinsmore, K.J., Smart, R.P., Garnett, M.H., Holden, J., Chapman, P., Baird, A.J., Grayson, R., & Stott, A.W. (2012). Variable source and age of different forms of carbon released from natural peatland pipes. *Journal of Geophysical Research: Biogeosciences*, 117, G02003. https://doi.org/10.1029/2011JG001807

Billett, M.F., Garnett, M.H., & Harvey, F. (2007). UK peatland streams release old carbon dioxide to the atmosphere and young dissolved organic carbon to rivers. *Geophysical Research Letters*, 34(23), L23401. https://doi.org/10.1029/2007GL031797

Billett, M.F., Palmer, S.M., Hope, D., Deacon, C., Storeton-West, R., Hargreaves, K.J., et al. (2004). Linking land-atmosphere-stream carbon fluxes in a lowland peatland system. *Global Biogeochemical Cycles*, 18 (1), GB1024. https://doi.org/10.1029/2003GB002058

Bogard, M.J., del Giorgio, P.A., Boutet, L., Chaves, M.C., Prairie, Y.T., Merante, A., & Derry, A.M. (2014). Oxic water column methanogenesis as a major component of aquatic CH_4 fluxes. *Nature Communications*, 5, 5350. https://doi.org/10.1038/ncomms6350

Bridgham, S.D., Cadillo-Quiroz, H., Keller, J.K., & Zhuang, Q. (2013). Methane emissions from wetlands: biogeochemical, microbial, and modeling perspectives from local to global scales. *Global Change Biology*, 19(5), 1325-1346.

Chanton, J.P., Glaser, P.H., Chasar, L.S., Burdige, D.J., Hines, M.E., Siegel, D.I., Tremblay, L.B., & Cooper, W.T. (2008). Radiocarbon evidence for the importance of surface vegetation on

fermentation and methanogenesis in contrasting types of boreal peatlands. *Global Biogeochemical Cycles*, 22(4), GB0422.

Chong, M., Humphreys, E., & Moore, T. R. (2012). Microclimatic response to increasing shrub cover and its effect on *Sphagnum* CO_2 exchange in a bog. *Ecoscience*, 19, 89-97. https://doi.org/10.2980/19-1-3489

Clark, J.M., Lane, S.N., Chapman, P.J., & Adamson, J.K. (2008). Link between DOC in near surface peat and stream water in an upland catchment. *Science of the Total Environment*, 404 (2-3), 308-315. https://doi.org/10.1016/j.scitotenv.2007.11.002

Cobb, A.R., Hoyt, A.M., Gandois, L., Eri, J., Dommain, R., Salim, K.A., et al. (2017). How temporal patterns in rainfall determine the geomorphology and carbon fluxes of tropical peatlands. *PNAS*, 114(26), E5187-E5196. https://doi.org/10.1073/pnas.1701090114

Coble, P.G. (2007). Marine optical biogeochemistry: The chemistry of ocean color. *Chemical Reviews*, 107(2), 402-418. https://doi.org/10.1002/chin.200720265

Cory, R.M., Ward, C.P., Crump, B.C., & Kling, G.W. (2014). Sunlight controls water column processing of carbon in arctic freshwaters. *Science*, 345(6199), 925-928.

D'Amario S.C., & Xenopoulos, M.A. (2015). Linking dissolved carbon dioxide to dissolved organic matter quality in streams. *Biogeochemistry*, 126, 99-114. https://doi.org/10.1007/s10533-015-0143-y

DelSontro, T., Boutet, L., St-Pierre, A., del Giorgio, P.A., & Prairie, Y. T. (2016). Methane ebullition and diffusion from northern ponds and lakes regulated by the interaction between temperature and system productivity. *Limnology and Oceanography*, 61, S62-S77. https://doi.org/10.1002/lno.10335

Dinsmore, K.J., Billett, M.F., Dyson, K.E., Harvey, F., Thomson, A.M., Piirainen, S., & Kortelainen, P. (2011). Stream water hydrochemistry as an indicator of carbon flow paths in Finnish peatland catchments during a spring snowmelt event. *Science of the Total Environment*, 409, 4858-4867. https://doi.org/10.1016/j.scitotenv.2011.07.063

Downing, J,A. (2009). Global limnology: up-scaling aquatic services and processes to the planet Earth. *Verhandlungen des Internationalen Verein Limnologie*, 30, 1149-1166. https://esajournals.onlinelibrary.wiley.com/journal/15409309

Downing, J.A., Cole, J.J., Duarte, C.M., Middelburg, J.J., Melack, J.M., Prairie, Y.T., et al. (2012). Global abundance and size distribution of streams and rivers. *Inland Waters*, 2(4), 229-236.

Downing, J.A., Prairie, Y., Cole, J., Duarte, C., Tranvik, L., Striegl, R. G., et al. (2006). The global abundance and size distribution of lakes, ponds, and impoundments. *Limnology and Oceanography*, 51(5), 2388-2397.

Einola, E., Rantakari, M., Kankaala, P., Kortelainen, P., Ojala, A., Pajunen, H., et al. (2011). Carbon pools and fluxes in a chain of five boreal lakes: a dry and wet year comparison. *Journal of Geophysical Research: Biogeosciences*, 116, G03009. https://doi.org/10.1029/2010JG001636

Fellman, J.B., Hood, E., Edwards, R.T., & Jones, J.B. (2009). Uptake of allochthonous dissolved organic matter from soil and salmon in coastal temperate rainforest streams. *Ecosystems*, 12, 747-759.

Fellman, J.B., D'Amore, D.V., Hood, E., & Boone, R.D. (2008). Fluorescence characteristics and biodegradability of dissolved organic matter in forest and wetland soils from coastal temperate watersheds in Southeast Alaska. *Biogeochemistry*, 88(2),169-184.

Feng, M., Sexton, J.O., Channan, S., & Townshend, J.R. (2016). A global, high-resolution (30-m) inland water body dataset for 2000: first results of a topographic–spectral classification algorithm. *International Journal of Digital Earth*, 9(2), 113-133. https://doi.org/10.1080/17538947.2015.1026420

Finlayson, C.M., & Milton, G.R. (2018). Peatlands. In: Finlayson, C., Milton, G., Prentice R. and Davidson, N. (eds). The Wetland Book. Springer, Dordrecht. https://doi.org/10.1007/978-94-007-4001-3_202

Freeman, C., Evans, C.D., Monteith, D.T., Reynolds, B., & Fenner, N. (2001). Export of organic carbon from peat soils. *Nature*, 412, 785. https://doi.org/10.1038/35090628

Frolking, S., & Roulet, N. (2007). Holocene radiative forcing impact of northern peatland carbon accumulation and methane emissions. *Global Change Biology*, 13, 1079-1088. https://doi.org/10.1111/j.1365-2486.2007.01339.x

Glaser, P.H. (1999). Patterned Mires and Mire Pools Patterned mires and mire pools–origin and development. In: Standen et. al. eds. (London: British Ecological Society) pp 55-65.

Guillemette, F., McCallister, S.L. & del Giorgio, P.A. (2015). Selective consumption and metabolic allocation of terrestrial and algal carbon determine allochthony in lake bacteria. *The ISME Journal*, 10, 1373-1382. https://doi.org/10.1038/ismej.2015.215

Hamilton, J.D., Kelly, C.A., Rudd, J.W.M., Hesslein, R.H., & Roulet, N.T. (1994). Flux to the atmosphere of CH_4 and CO_2 from wetland ponds on the Hudson Bay lowlands (HBLs). *Journal of Geophysical Research: Atmospheres*, 99, 1495-1510. https://doi.org/10.1029/93JD03020

Haraguchi, A., Iyobe, T., Nishijima, H., & Tomizawa, H. (2003). Acid and sea-salt accumulation in coastal peat mires of a *Picea glehnii* forest in Ochiishi, eastern Hokkaido, Japan. *Wetlands*, 23, 229-235. https://doi.org/10.1672/2-20

Helms, J.R., Stubbins, A., Ritchie, J.D., Minor, E.C., Kieber, D.J., & Mopper, K. (2006). *Absorption spectral slopes and slope ratios as indicators of molecular weight, sources, and photobleaching of chromophoric dissolved organic matter. Limnology and Oceanography*, 53(3), 955-969. https://doi.org/10.4319/lo.2008.53.3.0955

Holden, J., Moody, C.S., Turner T.E., McKenzie, R., Baird, A.J., Billett, M.F., Chapman, P.J., Dinsmore, K.J., Grayson, R.P., Andersen, R., Gee, C., & Dooling, G. (2018). Water-level dynamics in natural and artificial pools in blanket peatlands. *Hydrological Processes*, 32, 550-561.

Holgerson, M.A. (2015). Drivers of carbon dioxide and methane supersaturation in small temporary ponds. *Biogeochemistry*, 124, 305-318. https://doi.org/10.1007/s10533-015-0099-y

Holgerson, M.A., & Raymond, P.A. (2016). Large contribution to inland water CO_2 and CH_4 emissions from very small ponds. *Nature Geoscience*, 9, 222-226. https://doi.org/10.1038/ngeo2654

Holgerson, M.A., Farr, E.R., & Raymond, P.A. (2017). Gas transfer velocities in small forested ponds. *Journal of Geophysical Research: Biogeoscience*, 122, 1011-1021.

Hoyos-Santillan, J., Lomax, B.H., Large, D., Turner, B.L., Boom, A., Lopez, O.R., & Sjo¨gersten, S. (2015). Getting to the root of the problem: litter decomposition and peat formation in lowland Neotropical peatlands. *Biogeochemistry*, 126, 115-129.

Hoyos-Santillan, J., Lomax, B.H., Large, D., Turner, B.L., Boom, A., Lopez, O.R., & Sjögersten, S. (2016). Quality not quantity: organic matter composition controls of CO_2 and CH_4 fluxes in neotropical peat profiles. Soil Biology and Biochemistry, 103, 86-96. https://doi.org/10.1016/j.soilbio.2016.08.017

Iturraspe R. (2016). Patagonian Peatlands (Argentina and Chile). In C.M. Finlayson, G.R. Milton, R.C. Prentice, N.C. Davidson (eds.), *The Wetland Book* (pp.873-882). Dordrecht: Springer. https://doi.org/10.1007/978-94-007-4001-3

Jansson, M., Persson, L., De Roos, A.M., Roger I. Jones, R.I., & Tranvik, L.J. (2007). Terrestrial carbon and intraspecific size-variation shape lake ecosystems. *TRENDS in Ecology and Evolution*, 22, 316-322. https://doi.org/10.1016/j.tree.2007.02.015

Jonsson, A., Meili, M., Bergstrom, A-K., & Jansson, M. (2001). Whole lake mineralization of allochthonous and autochthonous organic carbon in a large humic lake (Ortrasket, N. Sweden). *Limnology and Oceanography*, 46, 1691-1700.

Juutinen, S., Rantakari, M., Kortelainen, P., Huttunen, J.T., Larmola, T., Alm, J., et al. (2009). Methane dynamics in different boreal lake types. *Biogeosciences*, 6, 209-223.

Kosten, S., Roland, F., Da Motta Marques, D.M.L., Van Nes, E.H., Mazzeo, N., Sternberg, L.D.S.L., et al. (2010). Climate-dependent CO_2 emissions from lakes. *Global Biogeochemical Cycles*, 24(2), GB2007. https://doi.org/10.1029/2009GB003618

Kritzberg, E.S., Cole, J.J., Pace, M.L., Grane´li, W., & Bade, D.L. (2004). Autochthonous versus allochthonous carbon sources of bacteria: Results from whole-lake ^{13}C addition experiments. *Limnology and Oceanography*, 49(2), 588-596. https://doi.org/10.4319/lo.2004.49.2.0588

Kuhn, M.A., Thompson, L.M., Winder, J.C., Braga, L.P.P., Tanentzap, A.J., Bastviken, D., & Olefeldt, D. (2021). Opposing effects of climate and permafrost thaw on CH_4 and CO_2 emissions from northern lakes. *AGU Advances*, 2(4), e2021AV000515. https://doi.org/10.1029/2021AV000515

Lambert, T., Teodoru, C.R., Nyoni, F.C., Bouillon, S., Darchambeau, F., Massicotte, P., & Borges, A.V. (2016). A long-stream transport and transformation of dissolved organic matter in a large tropical river. *Biogeosciences*, 13, 2727-2741. https://doi.org/10.5194/bg-13-2727-2016

Lapierre, J.-F., & del Giorgio P.A. (2014). Partial coupling and differential regulation of biologically and photo-chemically labile dissolved organic carbon across boreal aquatic networks. *Biogeosciences*, 11, 5969-5985. https://doi.org/10.5194/bg-11-5969-2014

Lapierre, J.-F., Collins, S.M., Seekell, D.A., Cheruvelil, K.S., Skaff, N.K., Taranu, Z.E., et al. (2018). Similarity in spatial structure constrains ecosystem relationships: Building a

macroscale understanding of lakes. *Global Ecology and Biogeography*, 27 (10), 1251-1263. https://doi.org/10.1111/geb.12781

Lapierre, J.-F**.**, Guillemette, F., Berggren, M., & del Giorgio P.A. (2013). Increases in terrestrially derived carbon stimulate organic carbon processing and CO_2 emissions in boreal aquatic ecosystems. *Nature Communications*, 4, 2972. https://doi.org/10.1038/ncomms3972

Lavoie, M., Colpron-Tremblay, J., & Robert, É.C. (2012). Développement d'une vaste tourbière ombrotrophe non perturbée en contexte périurbain au Québec méridional. *Ecoscience,* 19, 285-297. https://doi.org/10.2980/19-3-3538

Lehner, B., & Döll, P. (2004). Development and validation of a global database of lakes, reservoirs and wetlands. *Journal of Hydrology*, 296(1-4), 1-22.

Li, A., Aubeneau A.F., King, T., Cory, R.C., Neilson, B.T., Bolster, D., & Packman, A.I. (2019). Effects of Vertical Hydrodynamic Mixing on Photomineralization of Dissolved Organic Carbon in Arctic Surface Waters. *Environmental Science: Processes & Impacts*, 21, 748-760.

Li, Y., Harir, M., Lucio, M., Gonsior, M., Koch, B.P., Schmitt-Kopplin, P., & Hertkorn, N. (2016). Comprehensive structure-selective characterization of dissolved organic matter by reducing molecular complexity and increasing analytical dimensions. *Water Research*, 106, 477-487. https://doi.org/10.1016/j.watres.2016.10.034

Limpens, J., Berendse, F., Blodau, C., Canadell, J. G., Freeman, C., Holden, J., Roulet, N., Rydin, H., & Schaepman-Strub, G. (2008). Peatlands and the carbon cycle: from local processes to global implications - a synthesis. *Biogeosciences*, 5(5), 1475-1491.

Limpens, J., Granath, G., Gunnarsson, U., Aerts, R., Bayley, S., Bragazza, L., et al. (2011). Climatic modifiers of the response to nitrogen deposition in peat-forming *Sphagnum* mosses: A meta-analysis. *New Phytologist*, 191, 496-507. https://doi.org/10.1111/j.14698137.2011.03680.x

Lindsay, R. (2016). Peatland (Mire Types): Based on Origin and Behavior of Water, Peat Genesis, Landscape Position, and Climate. In: Finlayson, C., Milton, G., Prentice, R. and Davidson, N. (eds) *The Wetland Book*. Springer, Dordrecht. https://doi.org/10.1007/978-94-007-6173-5_279-1

Lou, T., & Xie, H. (2006). Photochemical alteration of the molecular weight of dissolved organic matter. *Chemosphere*, 65, 2333-2342.

McDonald, C.P., Rover, J.A., Stets, E.G., & Striegl, R.G. (2012). The regional abundance and size distribution of lakes and reservoirs in the United States and implications for estimates of global lake extent. *Limnology and Oceanography*, 57(2), 597-606.

McEnroe, N.A., Roulet, N.T., Moore, T.R., & Garneau, M. (2009). Do pool surface area and depth control CO_2 and CH_4 fluxes from an ombrotrophic raised bog, James Bay, Canada? *Journal of Geophysical Research: Biogeosciences*, 114, G01001. https://doi.org/10.1029/2007JG000639

McKenzie, J.M., Kurylyk, B.L., Walvoord, M.A., Bense, V.F., Fortier, D., Spence, C., & Grenier, C. (2021). Invited perspective: What lies beneath a changing arctic? *The Cryosphere*, *15*(1), 479-484. https://doi.org/10.5194/tc-15-479-2021

Messager, M.L., Lehner, B., Grill, G., Nedeva, I., & Schmitt, O. (2016). Estimating the volume and age of water stored in global lakes using a geo-statistical approach. *Nature Communications*, *7*, 1-11. https://doi.org/10.1038/ncomms13603

Michaud, A.B., Dore, J.E., Achberger, A.M., Christner, B.C., Mitchell, A.C., Skidmore, M. L., et al. (2017). Microbial oxidation as a methane sink beneath the West Antarctic Ice Sheet. *Nature Geoscience,* 10(8), 582-586. https://doi.org/10.1038/ngeo2992

Moore, S., Gauci, V., Evans, C.D., & Page, S.E. (2011). Fluvial organic carbon losses from a Bornean blackwater river. *Biogeosciences*, 8, 901-909.

Moore, T.R. (2009). Dissolved organic carbon production and transport in Canadian peatlands. In: Baird, A., Belyea, L., Comas, X., Reeve, A. and Slater, L. (Eds*.) Carbon cycling in northern peatlands*. AGU Geophysical Monograph, 184: 229-236. DOI:10.1029/2008GM000816.

Mostovaya, A., Hawkes, J.A., Dittmar, T., & Tranvik, L.J. (2017). Molecular determinants of dissolved organic matter reactivity in lake water. *Frontiers in Earth Science*, 5, 106.

Mullins, M.L., & Doyle, R.D. (2019). Big things come in small packages: why limnologists should care about small ponds. *Acta Limnologica Brasiliensia*, 31, 105.

Murphy, K.R., Stedmon, C.A., Graeberc, D., & Bro, R. (2013). Fluorescence spectroscopy and multi-way techniques PARAFAC. *Analytical Methods*, 5, 6557-6566. https://doi.org/10.1039/c3ay41160e

Murphy, K.R., Stedmon, C.A., Wenig, P., & Bro, R. (2014). OpenFluor- an online spectral library of auto-fluorescence by organic compounds in the environment. *Analytical Methods*, 6, 658-661. https://doi.org/10.1039/C3AY41935E

Natchimuthu, S., Selvam B.P., & Bastviken, D (2014). Influence of weather variables on methane and carbon dioxide flux from a shallow pond. *Biogeochemistry*, 119, 403-413. https://doi.org/10.1007/s10533-014-9976-z

Olefeldt, D., Hovemyr, M., Kuhn, M.A., Bastviken, D., Bohn, T.J., Connolly, J., et al. (2021). The boreal-arctic wetland and lake dataset (BAWLD). *Earth System Science Data*, 13(11), 5127-5149. https://doi.org/10.5194/essd-13-5127-2021

Page, S.E., Rieley, J.O., & Banks, C.J. (2011). Global and regional importance of the tropical peatland carbon pool. *Global Change Biology*, 17, 798-818.

Paytan, A., Lecher, A.L., Dimova, N., Sparrow, K.J., Kodovska, F. G.-T., Murray, J., et al. (2015). Methane transport from the active layer to lakes in the Arctic using Toolik Lake, Alaska, as a case study. *PNAS*, 112(12), 3636-3640. https://doi.org/10.1073/pnas.1417392112

Peacock, M., Audet, J., Jordan, S., Smeds, J., & Wallin, M.B. (2019). Greenhouse gas emissions from urban ponds are driven by nutrient status and hydrology. *Ecosphere*, 10(3), e02643. https://doi.org/10.1002/ecs2.2643

Pelletier, L., Strachan, I.B., Garneau, M., & Roulet, N.T. (2014). Carbon release from boreal peatland open water pools: implication for the contemporary C exchange. *Journal of Geophysical Research: Biogeosciences*, 119(3), 207-222. https://doi.org/10.1111/gcb.13815

Pelletier, L., Strachan, I.B., Roulet, N.T., & Garneau, M. (2015). Can boreal peatlands with pools be net sinks for CO_2? *Environmental Research Letters*, 10, 35002. https://doi.org/10.1088/1748-9326/10/3/035002

Pinsonneault, A.J., Moore, T.R., Roulet, N.T., & Lapierre, J.F. (2016). Biodegradability of vegetation-derived dissolved organic carbon in a cool temperate ombrotrophic bog. *Ecosystems*, 19, 1023-1036. https://doi.org/10.1007/s10021-016-9984-z.

Prairie, Y.T. (2008). Carbocentric limnology: looking back, looking forward. *Canadian Journal of Fisheries and Aquatic Sciences*, 65, 543-548. https://doi.org/10.1139/F08-011

Raymond, P.A., Hartmann, J., Lauerwald, R., Sobek, S., McDonald, C., Hoover, M., et al. (2013). Global carbon dioxide emissions from inland waters. *Nature*, 503, 355-359.

Repo, M.E., Huttunen, J.T., Naumov, A.V., Chichulin, A.V., Lapshina, E.D., Bleuten, W., & Martikainen, P.J. (2007). Release of CO_2 and CH_4 from small wetland lakes in western Siberia. *Tellus B*, 59, 788-796. https://doi.org/10.1111/j.1600-0889.2007.00301.x

Roehm, C.L., Prairie, Y.T., & del Giorgio, P.A. (2009). The pCO_2 dynamics in lakes in the boreal region of northern Quebec, Canada. *Global Biogeochemical Cycles*, 23(3), GB3013. https://doi.org/10.1029/2008GB003297

Rosentreter, J.A., Borges, A.V., Deemer, B.R., Holgerson, M.A., Liu, S., Song, C., et al. (2021). Half of global methane emissions come from highly variable aquatic ecosystem sources. *Nature Geoscience*, *14*(4), 225-230. https://doi.org/10.1038/s41561-021-00715-2

Roulet, N.T., Jano. A., Kelly, C.A., Klinger, L.F., Moore, T.R., Protz, R., Ritter, J.A., & Rouse, W.R. (1994). Role of the Hudson-Bay Lowland as a source of atmospheric methane. *Journal of Geophysical Research: Atmospheres*, 99, 1439-1454.

Sayer, E.J., & Tanner, E.V. (2010). A new approach to trenching experiments for measuring root–rhizosphere respiration in a lowland tropical forest. *Soil Biology and Biochemistry*, 42, 347-352.

Schlesinger, W.H., & Bernhardt, E.S. (2013). Wetland ecosystems. In: Schlesinger, W.H. and Bernhardt, E.S. (eds). *Biogeochemistry: An analysis of global change*. 3rd edition. Elsevier. 688pp.

Seekell, D.A., & Pace, M.L. (2011). Does the Pareto distribution adequately describe the size-distribution of lakes? *Limnology and Oceanography*, 56, 350-356.

Serikova, S., Pokrovsky, O.S., Laudon, H., Krickov, I.V., Lim, A.G., Manasypov, R.M., & Karlsson, J. (2019). High carbon emissions from thermokarst lakes of Western Siberia. *Nature Communications*, 10, 1552. https://doi.org/10.1038/s41467-019-09592-1

Sobek, S., Algesten, G., Bergstrom, A-K., Jansson, M., & Tranvik, L.J. (2003). The catchment and climate regulation of pCO2 in boreal lakes. *Global Change Biology*, 9, 630-641.

Sobek, S., Gudasz, C., Koehler, B., Tranvik, L.J., Bastviken, D., & Morales-Pineda, M. (2017). Temperature dependence of apparent respiratory quotients and oxygen penetration depth in contrasting lake sediments. *Journal of Geophysical Research: Biogeosciences*, 122, 3076-3087. https:// doi.org/10.1002/2017JG003833

Soranno, P.A., Cheruvelil, K., Liu, B., Wang, Q., Tan, P.N., Zhou, J., et al. (2020). Ecological prediction at macroscales using big data: Does sampling design matter? *Ecological Applications*, 30(6), e02123. https://doi.org/10.1002/eap.2123

Stanley, E.H., Casson, N.J., Christel, S.T., Crawford, J.T., Loken, L.C., & Oliver, S.K. (2016). The ecology of methane in streams and rivers: patterns, controls, and global significance. *Ecological Monographs*, 86(2), 146-171.

Stedmon, C.A., Markager, S., & Bro, R. (2003). Tracing dissolved organic matter in aquatic environments using a new approach to fluorescence spectroscopy. *Marine Chemistry*, 82, 239-254. https://doi.org/10.1016/S0304-4203(03)00072-0

Turner, T.E., Billett, M.F., Baird, A.J., Chapman, P.J., Dinsmore, K.J., & Holden, J. (2016). Regional variation in the biogeochemical and physical characteristics of natural peatland pools. *Science of the Total Environment*, 545-456, 84-94. https://doi.org/10.1016/j.scitotenv.2015.12.101

Verpoorter, C., Kutser, T., Seekell, D.A., & Tranvik, L.J. (2014). A global inventory of lakes based on high-resolution satellite imagery. *Geophysical Research Letters*, 41, 6396-6402.

Vizza, C., Zwart, J.A., Jones, S.E., Tiegs, S.D., & Lamberti, G.A. (2017). Landscape patterns shape wetland pond ecosystem function from glacial headwaters to ocean. *Limnology and Oceanography*, 62, S207-S221. https://doi.org/10.1002/lno.10575

Waddington, J.M., & Roulet, N.T. (2000). Carbon balance of a boreal patterned peatland. *Global Change Biology*, 6, 87-97. https://doi.org/10.1002/2013JG002423

Walker, S.A., Amon, R.M., & Stedmon, C.A. (2013). Variations in high latitude riverine fluorescent dissolved organic matter: A comparison of large Arctic rivers. *Journal of Geophysical Research: Biogeosciences*, 118, 1689-1702. https://doi.org/10.1002/2013JG002320

Wauthy, M., Rautio, M., Christoffersen, K.S., Forsstrom, L., Laurion, I., Mariash, H.L., et al. (2018). Increasing dominance of terrigenous organic matter in circumpolar freshwaters due to permafrost thaw. *Limnology and Oceanography Letters*, 3, 186-198. https://doi.org/10.1002/lol2.10063

Webb, J.R., Leavitt, P.R., Simpson, G.L., Baulch, H., Haig, H.A., Hodder, K.R., & Finlay, K. (2019). Regulation of carbon dioxide and methane in small agricultural reservoirs: Optimizing potential for greenhouse gas uptake. *Biogeosciences*, 16, 4211-4227.

Weishaar, J.L., Aiken, G.R., Bergamaschi, B.A., Fram, M.S., Fujii, R., & Mopper, K. (2003). Evaluation of specific ultraviolet absorbance as an indicator of the chemical composition

and reactivity of dissolved organic carbon. *Environmental Science and Technology*, 37, 4702-4708. https://doi.org/10.1021/es030360x

Weyhenmeyer, G. A., Kosten, S., Wallin, M. B., Tranvik, L. J., Jeppesen, E., & Roland, F. (2015). Significant fraction of CO_2 emissions from boreal lakes derived from hydrologic inorganic carbon inputs. *Nature Geoscience*, 8(12), 933-936. https://doi.org/10.1021/es030360x

Wik, M., Thornton, B. F., Bastviken, D., Macintyre, S., Varner, R. K., & Crill, P. M. (2014). Energy input is primary controller of methane bubbling in subarctic lakes. *Geophysical Research Letters,* 41, 555-560. https://doi.org/10.1002/2013GL058510

Wik, M., Varner, R.K., Anthony, K.W., MacIntyre, S., & Bastviken, D. (2016). Climate sensitive northern lakes and ponds are critical components of methane release. *Nature Geoscience*, 9(2), 99-105. https://doi.org/10.1038/ngeo2578

Xu, J., Morris, J., Liu, J., & Holden, J. (2018). PEATMAP: refining estimates of global peatlands distribution based on a meta-analysis. *Catena*, 160, 134-140.

Yamashita, Y., Boyer, J.N., & Jaffé, R., (2013). Evaluating the distribution of terrestrial dissolved organic matter in a complex coastal ecosystem using fluorescence spectroscopy. *Continental Shelf Research*, 66, 136-144. https://doi.org/10.1016/j.csr.2013.06.010.

Yamashita, Y., Jaffé, R., Maie, N., & Tanoue, E. (2008). Assessing the dynamics of dissolved organic matter (DOM) in coastal environments by excitation emission matrix fluorescence and parallel factor analysis (EEM-PARAFAC). *Limnology and Oceanography*, 53, 1900-1908. https://doi.org/10.4319/lo.2008.53.5.1900

Yu, Z., Beilman, D.W., Frolking, S., MacDonald, G.M., Roulet, N.T., Camill, P., & Charman, D.J. (2011). Peatlands and their role in the global carbon cycle. *EOS*, 92(12), 97-108. https://doi.org/10.1029/2011EO120001

Yu, Z.C., Loisel, J., Brosseau, D.P., Beilman, D.W., & Hunt, S.J. (2010). Global peatland dynamics since the Last Glacial Maximum. *Geophysical Research Letters*, 37(3), L13402.

Yvon-Durocher, G., Allen, A.P., Bastviken, D., Conrad, R., Gudasz, C., St-Pierre, A., et al. (2014). Methane fluxes show consistent temperature dependence across microbial to ecosystem scales. *Nature*, 507**,** 488-491. https://doi.org/10.1038/nature13164

Zhong, Y., Jiang, M., & Middleton, B.A. (2020). Effects of water level alteration on carbon cycling in peatlands. *Ecosystem Health and Sustainability*, 6(1), 1806113. https://doi.org/10.1080/20964129.2020.1806113

Zhou, Y., Xiao, Q., Yao, X., Zhang, Y., Zhang, M., Shi, K., et al. (2018). Accumulation of terrestrial dissolved organic matter potentially enhances dissolved methane levels in eutrophic Lake Taihu, China. *Environmental Science & Technology*, 52, 10297-10306. https://doi.org/10.1021/acs.est.8b02163